Huh-7 cells were transfected with a SPCS1-myc expression plasmid. Cell lysates of the transfected cells were immunoprecipitated with anti-myc antibody. The resulting precipitates and whole cell lysates used in immunoprecipitation (IP) were examined by immunoblotting using anti-NS2 or anti-SPCS1 antibody. (D) Expression of SPCS1-myc and its deletion mutants. 293T cells were transfected with indicated plasmids. The cell lysates were examined by immunoblotting using anti-myc or anti-actin antibody. (E) Cells were co-transfected with indicated plasmids, and then lysates of transfected cells were immunoprecipitated with anti-myc antibody. The resulting precipitates and whole cell lysates used in IP were examined by immunoblotting using anti-FLAG- or anti-myc antibody. (F) Lysates of the transfected cells were immunoprecipitated with anti-myc antibody. The resulting precipitates (right panel) and whole cell lysates used in IP (left panel) were examined by immunoblotting using anti-FLAG or anti-myc antibody. (G) 293T cells were transfected with indicated plasmids. 2 days posttransfection, cells were fixed and permeabilized with Triton X-100, then subjected to in situ PLA (Upper) or immunofluorescence staining (Lower) using anti-FLAG and anti-V5 antibodies. (H) Detection of the SPCS1-NS2 interaction in transfected cells using the mKG system. 293T cells were transfected by indicated pair of mKG fusion constructs. Twenty-four hours after transfection, cell were fixed and stained with DAPI, and observed under a confocal microscope.
doi:10.1371/journal.ppat.1003589.g001

absence of an expression plasmid for shRNA-resistant SPCS1 (SPCS1- sh^r). Western blotting confirmed the expression levels of SPCS1 in cells (Fig. 2D). As expected, viral production in the culture supernatants of the transfected cells was significantly impaired in SPCS1-knockdown cells compared with parental Huh-7 cells (Fig. 2E white bars). Expression of SPCS1- sh^r in KD#31 cells recovered virus production in the supernatant to a level similar to that in the parental cells. Expression of SPCS1-sh^r in parental Huh-7 cells did not significantly enhance virus production. Taken together, these results demonstrate that SPCS1 has an important role in HCV propagation, and that the endogenous expression level of SPCS1 is sufficient for the efficient propagation of HCV.

A typical feature of the *Flaviviridae* family is that their precursor polyprotein is processed into individual mature proteins mediated by host ER-resident peptidase(s) and viral-encoded protease(s). We therefore next examined the role of SPCS1 in the propagation of Japanese encephalitis virus (JEV), another member of the *Flaviviridae* family. SPCS1 siRNAs or control siRNA were transfected into Huh7.5.1 cells followed by infection with JEV or HCVcc. Although knockdown of SPCS1 severely impaired HCV production (Fig. 3A), the propagation of JEV was not affected under the SPCS1-knockdown condition (Fig. 3B). Expression of the viral proteins as well as knockdown of SPCS1 were confirmed (Fig. 3C). This suggests that SPCS1 is not a broadly active modulator of the flavivirus lifecycle, but rather is involved specifically in the production of certain virus(es) such as HCV.

Knockdown of SPCS1 exhibits no influence on the processing of HCV proteins and the secretion of host-cell proteins

Since SPCS1 is a component of the signal peptidase complex, which plays a role in proteolytic processing of membrane proteins at the ER, it may be that SPCS1 is involved in processing HCV

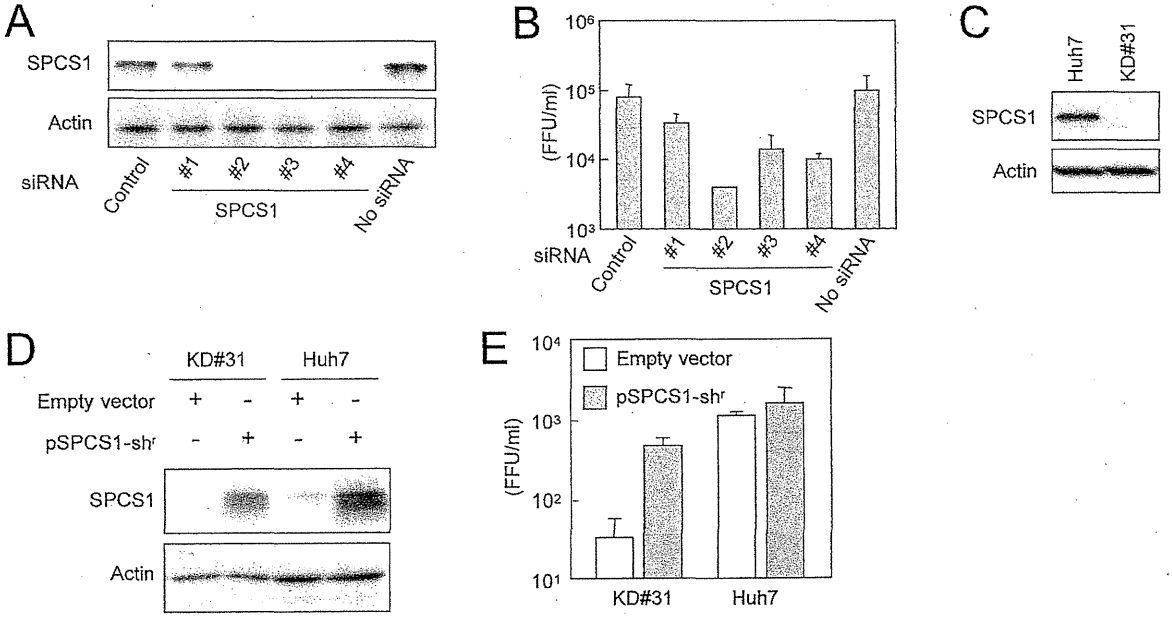

Figure 2. Effect of SPCS1 knockdown on the production of HCV. (A) Huh7.5.1 cells were transfected with four different siRNAs targeted for SPCS1 or control siRNA at a final concentration of 15 nM, and infected with HCVcc at a multiplicity of infection (MOI) of 0.05 at 24 h post-transfection. Expression levels of endogenous SPCS1 and actin in the cells were examined by immunoblotting using anti-SPCS1 and anti-actin antibodies at 3 days post-infection. (B) Infectious titers of HCVcc in the supernatant of cells infected as above were determined at 3 days postinfection. (C) Huh-7 cells were transfected with pSilencer-SPCS1, and hygromycin B-resistant cells were selected. The SPCS1-knockdown cell line established (KD#31) and parental Huh-7 cells were subjected to immunoblotting to confirm SPCS1 knockdown. (D) KD#31 cells or parental Huh-7 cells were transfected with RNA pol I-driven full-length HCV plasmid in the presence or absence of shRNA-resistant SPCS1 expression plasmid. Expression levels of SPCS1 and actin in the cells at 5 days post-transfection were examined by immunoblotting using anti-SPCS1 and anti-actin antibodies. (E) Infectious titers of HCVcc in the supernatants of transfected SPCS1-knockdown cells or parental Huh-7 cells at 5 days post-transfection were determined.
doi:10.1371/journal.ppat.1003589.g002

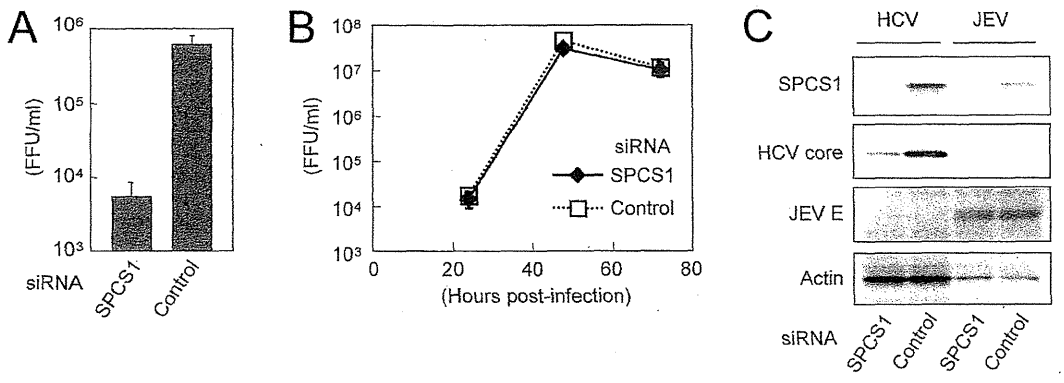

Figure 3. Effect of SPCS1 knockdown on the propagation of JEV. Huh7.5.1 cells were transfected with SPCS1 siRNA or control siRNA at a final concentration of 10 nM, and infected with JEV or HCVcc at an MOI of 0.05 at 24 h post-transfection. (A) Infectious titers of HCVcc in the supernatant at 3 days post-infection were determined. (B) Infectious titers of JEV in the supernatant at indicated time points were determined. (C) Expression levels of endogenous SPCS1 and actin as well as viral proteins in the cells were determined by immunoblotting using anti-SPCS1, anti-actin, anti-HCV core, and anti-JEV antibodies 3 days post-infection.
doi:10.1371/journal.ppat.1003589.g003

proteins via interacting with ER membranes. To address this, the effect of SPCS1 knockdown on the processing of HCV precursor polyproteins in cells transiently expressing the viral Core-NS2 region was analyzed. Western blotting indicated that properly processed core and NS2 were observed in KD#31 cells as well as Huh-7 cells (Fig. 4A). No band corresponding to the unprocessed precursor polyprotein was detected in either cell line (data not shown). We also examined the effect of SPCS1 knockdown on the cleavage of the NS2/3 junction mediated by NS2/3 protease. Processed NS2 was detected in both cell lines with and without SPCS1 knockdown, which were transfected with wild-type or protease-deficient NS2-3 expression plasmids (Fig. 4B & C).

Signal peptidase plays a key role in the initial step of the protein secretion pathway by removing the signal peptide and releasing the substrate protein from the ER membrane. It is now accepted that the secretion pathways of very-low density lipoprotein or apolipoprotein E (apoE) are involved in the formation of infectious HCV particles and their release from cells [34,35]. ApoE is synthesized as a pre-apoE. After cleavage of its signal peptide in the ER, the protein is trafficked to the Golgi and trans-Golgi network before being transported to the plasma membrane and secreted. As shown in Fig. 4D, the secreted levels of apoE from Huh-7 cells with knocked-down of SPCS1 were comparable to those from control cells. In addition, the level of albumin, an abundant secreted protein from hepatocytes, in the culture supernatants of the cells was not influenced by SPCS1 knockdown (Fig. 4E). These data suggest that the knockdown of SPCS1 has no influence on the processing of viral and host secretory proteins by signal peptidase and HCV NS2/3 protease.

SPCS1 is involved in the assembly process of HCV particles but not in viral entry into cells and RNA replication

To further address the molecular mechanism(s) of the HCV lifecycle mediated by SPCS1, we examined the effect of SPCS1 knockdown on viral entry and genome replication using single-round infectious trans-complemented HCV particles (HCVtcp) [33], of which the packaged genome is a subgenomic replicon containing a luciferase reporter gene. This assay system allows us to evaluate viral entry and replication without the influence of reinfection. Despite efficient knockdown of SPCS1 (Fig. 5A), luciferase activity expressed from HCVtcp in SPCS1-knockdown cells was comparable to that in control or non-siRNA-transfected cells (Fig. 5B), suggesting that SPCS1 is not involved in viral entry into cells and subgenomic RNA replication. As a positive control, knockdown of claudin-1, a cell surface protein required for HCV entry, reduced the luciferase activity. We also examined the effect of SPCS1 knockdown on full-genome replication using HCVcc-infected cells. Despite efficient knockdown of SPCS1, expression of HCV proteins was comparable to that in control cells (Fig. 5C). By contrast, knockdown of PI4 Kinase (PI4K), which is required for replication of HCV genome, led to decrease in expression of HCV proteins. As cells that had already been infected with HCV were used, knockdown of claudin-1 had no effect on HCV protein levels. These data suggest that SPCS1 is not involved in viral entry into cells and the viral genome replication. We also observed properly processed Core, E2, NS2 and NS5B in SPCS1-knockdown cells in consistent with the result as shown in Fig. 4A, indicating no effect of SPCS1 on HCV polyprotein processing.

Next, to investigate whether SPCS1 is involved in the assembly or release of infectious particles, SPCS1-shRNA plasmid along with a pol I-driven full-genome HCV plasmid [33] were transfected into CD81-negative Huh7-25 cells, which can produce infectious HCV upon introduction of the viral genome, but are not permissive to HCV infection [36]. It is therefore possible to examine viral assembly and the release process without viral reinfection. The infectivity within the transfected cells as well as supernatants was determined 5 days post-transfection. Interestingly, both intra- and extracellular viral titers were markedly reduced by SPCS1 knockdown (Fig. 5C).

Taken together, in the HCV lifecycle, SPCS1 is most likely involved in the assembly of infectious particles rather than cell entry, RNA replication, or release from cells.

Role of SPCS1 in complex formation between NS2 and E2

It has been shown that HCV NS2 interacts with the viral structural and NS proteins in virus-producing cells [18–21], and that some of the interactions, especially the NS2-E2 interaction, are important for the assembly of infectious HCV particles. However, the functional role of NS2 in the HCV assembly process has not been fully elucidated. To test whether SPCS1 is involved in the interaction between NS2 and E2, cells were co-transfected

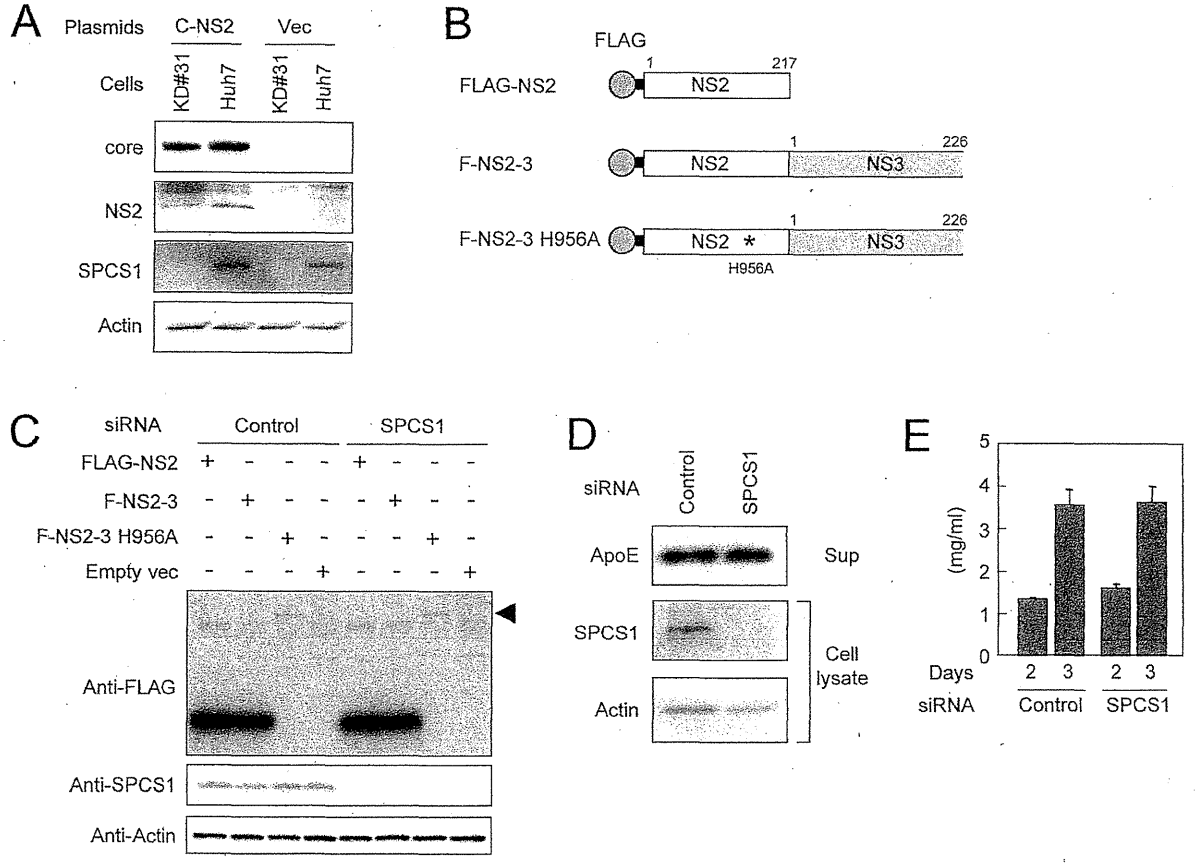

Figure 4. Effect of SPCS1 knockdown on the processing of HCV structural proteins and secretion of host proteins. (A) Core-NS2 polyprotein was expressed in KD#31 cells or parental Huh-7 cells. Core, NS2, SPCS1, and actin were detected by immunoblotting 2 days post-transfection. (B) Expression constructs of NS2 and NS2/3 proteins. His to Ala substitution mutation at aa 956 in NS2 is indicated by an asterisk. Gray circles and bold lines indicate FLAG-tag and the spacer sequences, respectively. Positions of the aa residues are indicated above the boxes. (C) Effect of SPCS1 knockdown on processing at the NS2/3 junction. Huh-7 cells were transfected with SPCS1 siRNA or control siRNA at a final concentration of 30 nM, and then transfected with plasmids for FLAG-NS2, F-NS2-3, or F-NS2-3 with a protease-inactive mutation (H956A). NS2 in cell lysates was detected by anti-FLAG antibody 2 days post-transfection. Arrowhead indicates unprocessed NS2-3 polyproteins. (D) Effect of SPCS1 knockdown on the secretion of apoE. Huh7.5.1 cells were transfected with SPCS1 siRNAs or control siRNA at a final concentration of 20 nM, and apoE in the supernatant and SPCS1 and actin in the cells were detected 3 days post-transfection. (E) Effect of SPCS1 knockdown on the secretion of albumin. Huh7.5.1 cells were transfected with SPCS1 siRNA or control siRNA, and albumin in the culture supernatants at 2 and 3 days post-transfection was measured by ELISA.

doi:10.1371/journal.ppat.1003589.g004

with expression plasmids for E2, FLAG-NS2, and SPCS1-myc. E2 and NS2 were co-immunoprecipitated with SPCS1-myc, and E2 and SPCS1-myc were co-immunoprecipitated with FLAG-NS2 (Fig. 6A), suggesting the formation of an E2-NS2-SPCS1 complex in cells. To investigate the interaction of SPCS1 with E2 in the absence of NS2, HCV Core-p7 polyprotein or E2 protein were co-expressed with SPCS1-myc in cells, followed by immunoprecipitation with anti-myc antibody. As shown in Fig. 6B and Fig. S2, E2 was co-immunoprecipitated with SPCS1-myc. The interaction between SPCS1 and E2 was further analyzed *in situ* by PLA and mKG system. Specific signals indicating formation of the SPCS1-E2 complex were detected in both assays (Fig. S3), suggesting physical interaction between SPCS1 and E2 in cells.

We further determined the region of SPCS1 responsible for the interaction with E2 by co-immunoprecipitation assays. Full-length and deletion mutant d2 of SPCS1 (Fig. 1A) were similarly co-immunoprecipitated with E2, while only a limited amount of d1 mutant SPCS1 (Fig. 1A) was co-precipitated (Fig. 6C). It may be that the aa 43–102 region of SPCS1, which was identified as the region involved in the NS2 interaction (Fig. 1D), is important for its interaction with E2, and that deletion of the N-terminal cytoplasmic region leads to misfolding of the protein and subsequent inaccessibility to E2.

Finally, to understand the significance of SPCS1 in the NS2-E2 interaction, Huh7.5.1 cells with or without SPCS1 knockdown by siRNA were transfected with expression plasmids for Core-p7 and FLAG-NS2, followed by co-immunoprecipitation with anti-FLAG antibody. As shown in Fig. 6D, the NS2-E2 interaction was considerably impaired in the SPCS1-knockdown cells as compared to that in the control cells. A similar result was obtained in the stable SPCS1-knockdown cell line (Fig. 6E). In contrast, in that cell line, the interaction of NS2 with NS3 was not impaired by SPCS1 knockdown (Fig. 6E).

These results, together with the above findings, suggest that SPCS1 is required for or facilitates the formation of the membrane-associated NS2-E2 complex, which participates in the proper assembly of infectious particles.

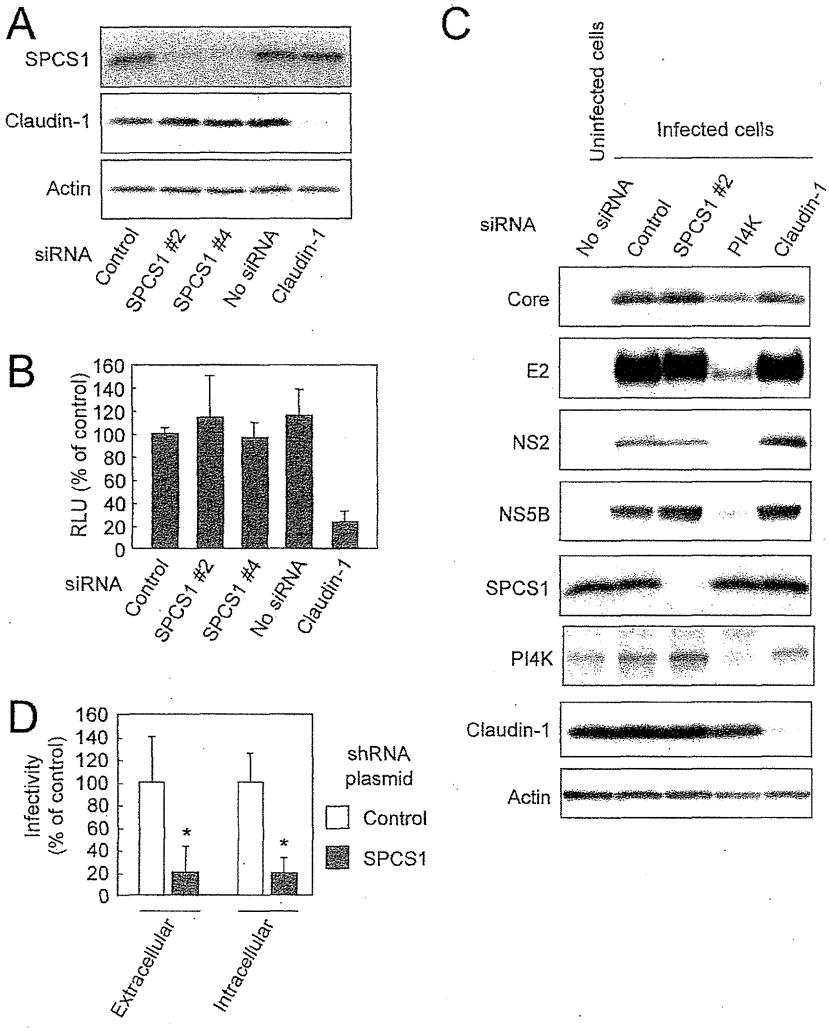

Figure 5. Effect of SPCS1 knockdown on entry into cells, genome replication, and assembly or release of infectious virus. (A) Huh7.5.1 cells were transfected with siRNA for SPCS1 or claudin1, or control siRNA at a final concentration of 30 nM. Expression levels of endogenous SPCS1, claudin-1, and actin in the cells at 2 days post-transfection were examined by immunoblotting using anti-SPCS1, anti-actin, and anti-claudin-1 antibodies. (B) Huh7.5.1 cells transfected with indicated siRNAs were infected with HCVtcp at 2 days post-transfection. Luciferase activity in the cells was subsequently determined at 2 days post-infection. Data are averages of triplicate values with error bars showing standard deviations. (C) Effect of SPCS1 knockdown on replication of HCV genome. HCV-infected Huh-7 cells transfected with siRNA for SPCS1, PI4K or claudin1, or control siRNA at a final concentration of 30 nM. Expression levels of HCV proteins as well as endogenous SPCS1, PI4K, claudin-1, and actin in the cells at 3 days post-transfection were examined by immunoblotting. (D) HCV infectivity in Huh7.5.1 cells inoculated with culture supernatant and cell lysate from Huh7-25 cells transfected with pSilencer-SPCS1 or control vector along with pHH/JFH1am at 5 days post-transfection. Statistical differences between Control and SPCS1 knockdown were evaluated using Student's t-test. *$p<0.005$ vs. Control.
doi:10.1371/journal.ppat.1003589.g005

Discussion

In this study, we identified SPCS1 as a novel host factor that interacts with HCV NS2, and showed that SPCS1 participates in HCV assembly through complex formation with NS2 and E2. In general, viruses require host cell-derived factors for proceeding and regulating each step in their lifecycle. Although a number of host factors involved in genome replication and cell entry of HCV have been reported, only a few for viral assembly have been identified to date. To our knowledge, this is the first study to identify an NS2-interacting host protein that plays a role in the production of infectious HCV particles.

NS2 is a hydrophobic protein containing TM segments in the N-terminal region. The C-terminal half of NS2 and the N-terminal third of NS3 form the protease, which is a prerequisite for NS2-NS3 cleavage. In addition, it is now accepted that this protein is essential for particle production [4–6,12]. However, the mechanism of how NS2 is involved in the assembly process of HCV has been unclear.

So far, two studies have screened for HCV NS2 binding proteins by yeast two-hybrid analysis [37,38]. Erdtmann et al. reported that no specific interaction was detected by a conventional yeast hybrid screening system using full-length NS2 as a bait, probably due to hampered translocation of the bait to the

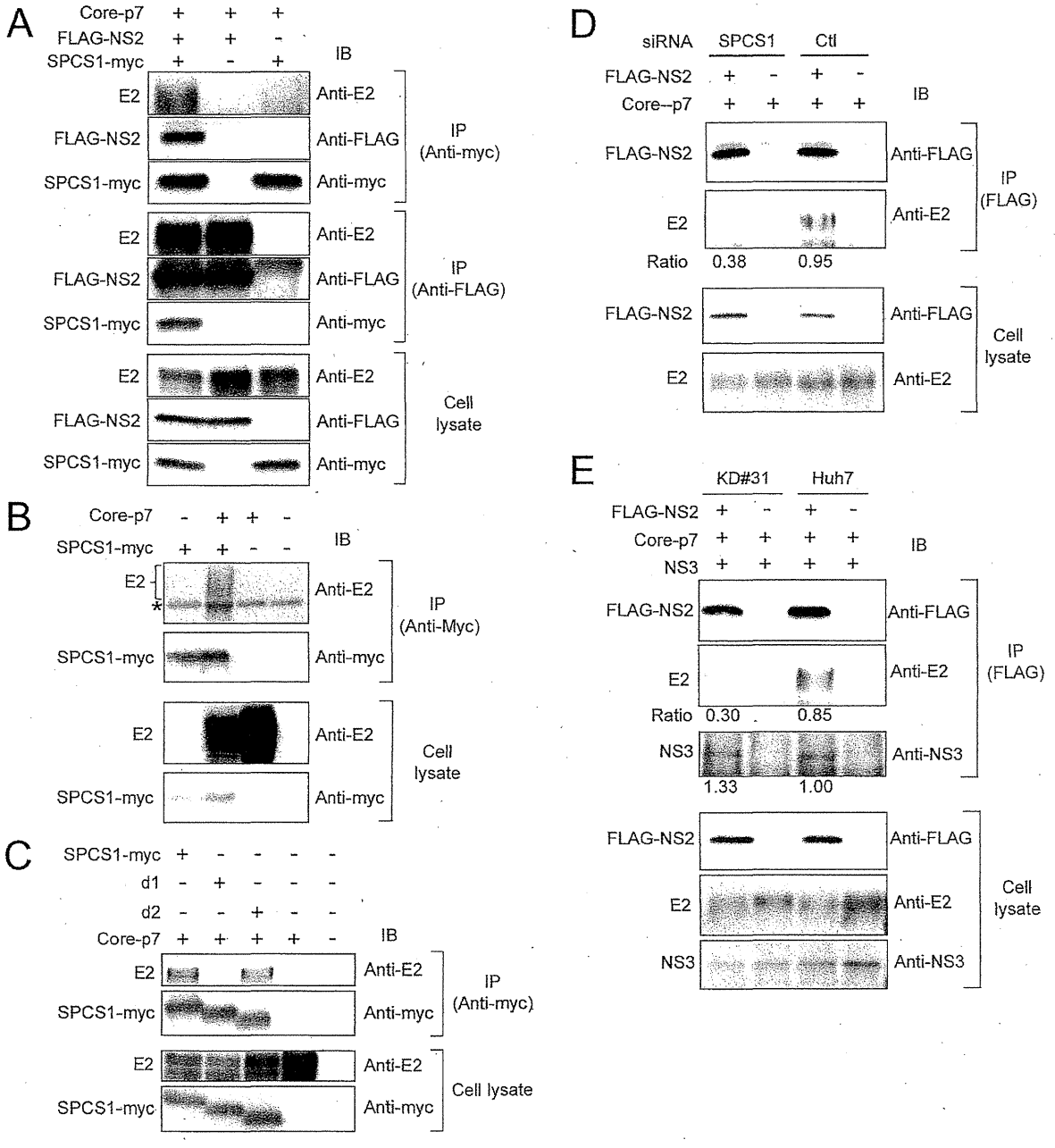

Figure 6. SPCS1 forms a complex with NS2 and E2. (A) Lysates of cells, which were co-transfected with Core-p7, FLAG-NS2, and SPCS1-myc expression plasmids, were immunoprecipitated with anti-myc or anti-FLAG antibody. The resulting precipitates and whole cell lysates used in IP were examined by immunoblotting using anti-E2, anti-FLAG, or anti-myc antibody. An empty plasmid was used as a negative control. (B) Cells were transfected with Core-p7 expression plasmid in the presence or absence of SPCS1-myc expression plasmid. The cell lysates of the transfected cells were immunoprecipitated with anti-myc antibody. The resulting precipitates and whole cell lysates used in IP were examined by immunoblotting using anti-E2 or anti-myc antibody. An empty plasmid was used as a negative control. The bands corresponding to immunoglobulin heavy chain are marked by an asterisk. (C) Cells were co-transfected with Core-p7 and SPCS1-myc expression plasmids. The cell lysates of the transfected cells were immunoprecipitated with anti-myc antibody. The resulting precipitates and whole cell lysates used in IP were examined by immunoblotting using anti-E2 or anti-myc antibody. (D) Huh7.5.1 cells were transfected with SPCS1 siRNA or control siRNA at a final concentration of 20 nM. After 24 h, Huh7.5.1 cells were then co-transfected with FLAG-NS2 and Core-p7 expression plasmids. The lysates of transfected cells were immunoprecipitated with anti-FLAG antibody, followed by immunoblotting with anti-FLAG and anti-E2 antibodies. Immunoblot analysis of whole cell lysates was also performed. Intensity of E2 bands was quantified, and the ratio of immunoprecipitated E2 to E2 in cell lysate was shown. Similar results were obtained in 2 independent experiments. (E) KD#31 cells and parental Huh-7 cells were co-transfected with FLAG-NS2, Core-p7, and NS3 expression plasmids. The lysates of transfected cells were immunoprecipitated with anti-FLAG antibody followed by immunoblotting with anti-FLAG, anti-E2, and anti-NS3 antibodies. Immunoblot analysis of whole cell lysates was also performed. The ratio of immunoprecipitated E2 or NS3 to E2 or NS3 in cell lysate, respectively, were shown.

doi:10.1371/journal.ppat.1003589.g006

nucleus [37]. They further screened a human liver cDNA library using NS2 with deletion of the N-terminal TM domain, and CIDE-B protein, a member of the CIDE family of apoptosis-inducing factors, was identified. However, whether CIDE-B is involved in the HCV lifecycle and/or viral pathogenesis is unclear. de Chassey et al. reported several cellular proteins as potential NS2 binding proteins using NS2 with N-terminal deletion as a bait [38]. Involvement of these proteins in the HCV lifecycle is also unclear. In our study, to screen for NS2-binding partners using full-length NS2 as a bait, we utilized a split-ubiquitin yeast two-hybrid system that allows for the identification of interactions between full-length integral membrane proteins or between a full-length membrane-associated protein and a soluble protein [39]. SPCS1 was identified as a positive clone of an NS2-binding protein, but proteins that have been reported to interact with NS2 were not selected from our screening.

SPCS1 is a component of the signal peptidase complex that processes membrane-associated and secreted proteins in cells. The mammalian signal peptidase complex consists of five subunits, SPCS1, SPCS2, SPCS3, SEC11A, and SEC11C [27]. Among them, the functional role of SPCS1 is still unclear, and SPCS1 is considered unlikely to function as a catalytic subunit according to membrane topology [40]. The yeast homolog of SPCS1, Spc1p, is also known to be nonessential for cell growth and enzyme activity [28,41]. Interestingly, these findings are consistent with the results obtained in this study. Knockdown of SPCS1 did not impair processing of HCV structural proteins (Fig. 4A) or secretion of apoE and albumin (Fig. 4B and C), which are regulated by ER membrane-associated signal peptidase activity. The propagation of JEV, whose structural protein regions are cleaved by signal peptidase, was also not affected by the knockdown of SPCS1 (Fig. 3B). SPCS1, SPCS2, and SPCS3 are among the host factors that function in HCV production identified from genome-wide siRNA screening [42]. It seemed that knockdown of SPCS1 had a higher impact on the later stage of viral infection compared to either SPCS2 or SPCS3, which are possibly involved in the catalytic activity of the signal peptidase.

Further analyses to address the mechanistic implication of SPCS1 on the HCV lifecycle revealed that SPCS1 knockdown impaired the assembly of infectious viruses in the cells, but not cell entry, RNA replication, or release from the cells (Fig. 5). We thus considered the possibility that the SPCS1-NS2 interaction is important for the role of NS2 in viral assembly. Several studies have reported that HCV NS2 is associated biochemically or genetically with viral structural proteins as well as NS proteins [10,18–25]. As an intriguing model, it has been proposed that NS2 functions as a key organizer of HCV assembly and plays a key role in recruiting viral envelope proteins and NS protein(s) such as NS3 to the assembly sites in close proximity to lipid droplets [21]. The interaction of NS2 with E2 has been shown by use of an HCV genome encoding tagged-NS2 protein in virion-producing cells. Furthermore, the selection of an assembly-deficient NS2 mutation located within its TM3 for pseudoreversion leads to a rescue mutation in the TM domain of E2, suggesting an in-membrane interaction between NS2 and E2 [21]. Another study identified two classes of NS2 mutations with defects in virus assembly; one class leads to reduced interaction with NS3, and the other, located in the TM3 domain, maintains its interaction with NS3 but shows impaired interaction between NS2 and E1-E2 [20]. However, the precise details of the NS2-E2 interaction, such as direct protein-protein binding or participating host factors, are unknown. Our results provide evidence that SPCS1 has an important role in the formation of the NS2-E2 complex by its interaction with both NS2 and E2, most likely via their transmembrane domains, including TM3 of NS2. As knockdown of SPCS1 reduced the interaction of NS2 and E2 as shown in Fig. 6D and E, it may be that SPCS1 contributes to NS2-E2 complex formation or to stabilizing the complex. Based on data obtained in this study, we propose a model of the formation of an E2-SPCS1-NS2 complex at the ER membrane (Fig. 7).

In summary, we identified SPCS1 as a novel NS2-binding host factor required for HCV assembly by split-ubiquitin membrane yeast two-hybrid screening. Our data demonstrate that SPCS1 plays a key role in the E2-NS2 interaction via formation of an E2-SPCS1-NS2 complex. These findings provide clues for understanding the molecular mechanism of assembly and formation of infectious HCV particles.

Materials and Methods

Split ubiquitin-based yeast two-hybrid screen

A split-ubiquitin membrane yeast two-hybrid screen was performed to identify possible NS2 binding partners. This screening system (DUALmembrane system; Dualsystems Biotech, Schlieren, Switzerland) is based on an adaptation of the ubiquitin-based split protein sensor [26]. The full-length HCV NS2 gene derived from the JFH-1 strain [29] was cloned into pBT3-SUC bait vector to obtain bait protein fused to the C-terminal half of ubiquitin (NS2-Cub) along with a transcription factor. Prey proteins generated from a human liver cDNA library (Dualsystems Biotech) were expressed as a fusion to the N-terminal half of ubiquitin (NubG). Complex formation between NS2-Cub and NubG-protein from the library leads to cleavage at the C-terminus of reconstituted ubiquitin by ubiquitin-specific protease(s) with consequent translocation of the transcription factor into the nucleus. Library plasmids were recovered from positive transformants, followed by determining the nucleotide sequences of inserted cDNAs, which were identified using the BLAST algorithm with the GenBank database.

Cell culture

Human embryonic kidney 293T cells, and human hepatoma Huh-7 cells and its derivative cell lines Huh7.5.1 [43] and Huh7-25 [36], were maintained in Dulbecco's modified Eagle medium supplemented with nonessential amino acids, 100 U of penicillin/ml, 100 μg of streptomycin/ml, and 10% fetal bovine serum (FBS) at 37°C in a 5% CO_2 incubator.

Plasmids

Plasmids pCAGC-NS2/JFH1am and pHHJFH1am were previously described [33]. The plasmid pCAGC-p7/JFHam, having

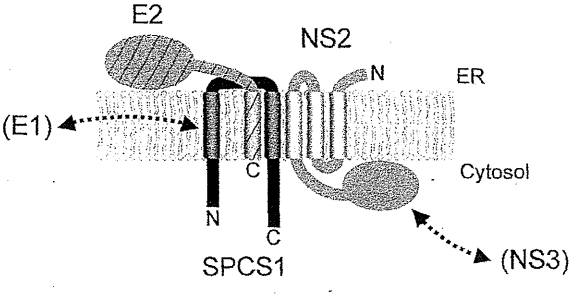

Figure 7. A proposed model for a complex consisting of NS2, SPCS1 and E2 associated with ER membranes.
doi:10.1371/journal.ppat.1003589.g007

adaptive mutations in E2 (N417S) and p7 (N765D) in pCAG/C-p7 [44], was constructed by oligonucleotide-directed mutagenesis.

To generate the NS2 expression plasmid pCAG F-NS2 and the NS2-deletion mutants, cDNAs encoding the full-length or parts of NS2 possessing the FLAG-tag and spacer sequences (MDYKDDDDKGGGGS) were amplified from pCAGC-NS2/JFH1am by PCR. The resultant fragments were cloned into pCAGGS. For the NS2-NS3 expression plasmid pEF F-NS2-3, a cDNA encoding the entire NS2 and the N-terminal 226 amino acids of NS3 with the N-terminal FLAG-tag sequence as above was amplified by PCR and was inserted into pEF1/myc-His (Invitrogen, Carlsbad, CA). The plasmid pEF F-NS2-3 H956A, having a defective mutation in the protease active site within NS2, was constructed by oligonucleotide-directed mutagenesis.

To generate the NS3 expression plasmid pCAGN-HANS3JFH1, a cDNA encoding NS3 with an HA tag at the N terminus, which was amplified by PCR with pHHJFHam as a template, was inserted downstream of the CAG promoter of pCAGGS.

To generate the SPCS1-expressing plasmid pCAG-SPCS1-myc and its deletion mutants, cDNAs encoding all of or parts of SPCS1 with the Myc tag sequence (EQKLISEEDL) at the C-terminus, which was amplified by PCR, was inserted into pCAGGS. pSilencer-shSPCS1 carrying a shRNA targeted to SPCS1 under the control of the U6 promoter was constructed by cloning the oligonucleotide pair 5′- GATCCGCAATAGTTGGATTTATCTTTCAAGAGAAGATAAATCCAACTATTGCTTTTTTGGAAA-3′ and 5′- AGCTTTTCCAAAAAAGCAATAGTTGGATTTATCTTCTCTTGAAAGATAAATCCAACTATTGCG-3′ between the BamHI and HindIII sites of pSilencer 2.1-U6 hygro (Ambion, Austin, TX). To generate a construct expressing shRNA-resistant SPCS1 pSPCS1-sh^r, a cDNA fragment coding for SPCS1, in which the 6 bp within the shRNA targeting region (5′-GCAATAGTTGGATTTATCT-3′) was replaced with GCTATTGTCGGCTTCATAT that causes no aa change, was amplified by PCR. The resulting fragment was confirmed by sequencing and then cloned into pCAGGS.

Full-length SPCS1 and N-terminal region of NS2 (aa 1–94) were amplified by PCR and cloned onto EcoRI and HindIII sites of phmKGN-MN and phmKGC-MN, which encode the mKG fragments (CoralHue Fluo-chase Kit; MBL, Nagoya, Japan), designated as pSPCS1-mKG(N) and pNS2-mKG(C), respectively. Transmembrane domain of the E1 to E2 was also amplified by PCR and cloned onto EcoRI and HindIII sites of phmKGC-MN. To avoid the cleavage of E2-mKG(C) fusion protein in the cells, last alanine of the E2 protein was deleted. Positive control plasmids for mKG system, pCONT-1 and pCONT-2, which encode p65 partial domain from NF-κB complex fused to mKG(N) and p50 partial domain from NF-κB complex fused to mKG(C) respectively, were supplied from MBL. For PLA experiments, cDNA for SPCS1 d2-myc with the V5 tag at the N-terminus was amplified by PCR, and inserted into pCAGGS. For expression of HCV E2, cDNA from E1 signal to the last codon of the transmembrane domain of the E2, in which part of the hypervariable region-1 (aa 394–400) were replaced with FLAG-tag and spacer sequences (DYKDDDDKGGG), was amplified by PCR, and inserted into pCAGGS. For expression of FLAG-core, cDNAs encoding Core (aa 1–152) possessing the FLAG-tag and spacer sequences (MDYKDDDDKGGGGS) were amplified from pCAGC191 [45] by PCR. The resultant fragments were cloned into pCAGGS.

DNA transfection

Monolayers of 293T cells were transfected with plasmid DNA using FuGENE 6 transfection reagent (Roche, Basel, Switzerland) in accordance with the manufacturer's instructions. Huh-7, Huh7.5.1, and Huh7-25 cells were transfected with plasmid DNA using TransIT LT1 transfection reagent (Mirus, Madison, WI).

PLA

The assay was performed in a humid chamber at 37°C according to the manufacturer's instructions (Olink Bioscience, Uppsala, Sweden). Transfected 293T cells were grown on glass coverslips. Two days after transfection, cells were fixed with 4% paraformaldehyde in phosphate-buffered saline (PBS) for 20 min, then blocked and permeabilized with 0.3% Triton X-100 in a nonfat milk solution (Block Ace; Snow Brand Milk Products Co., Sapporo, Japan) for 60 min at room temperature. Then the samples were incubated with a mixture of mouse anti-FLAG monoclonal antibody M2 and rabbit anti-V5 polyclonal antibody for 60 min, washed three times, and incubated with plus and minus PLA probes. After washing, the ligation mixture containing connector oligonucleotide was added for 30 min. The washing step was repeated, and amplification mixture containing fluorescently labeled DNA probe was added for 100 min. Finally, the samples were washed and mounted with DAPI mounting medium. The signal representing interaction was analyzed by Leica TCS SPE confocal microscope.

mKG system

The assay was performed according to the manufacturer's instructions (CoralHue Fluo-chase Kit; MBL). 293T cells were transfected by a pair of mKG fusion constructs. Twenty-four hours after transfection, cell were fixed and stained with DAPI. The signal representing interaction was analyzed by Leica TCS SPE confocal microscope.

Gene silencing by siRNA

The siRNAs were purchased from Sigma-Aldrich (St. Louis, MO) and were introduced into the cells at a final concentration of 10 to 30 nM using Lipofectamine RNAiMAX (Invitrogen). Target sequences of the siRNAs were as follows: SPCS1 #1 (5′-CAGUUCGGGUGGACUGUCU-3′), SPCS1 #2 (5′-GCAAUAGUUGGAUUUAUCU-3′), SPCS1 #3 (5′-GAUGUUUCAGGGAAUUAUU-3′), SPCS1 #4 (5′-GUUAUGGCCGGAUUUGCUU-3′), claudin-1 (5′-CAGUCAAUGCCAGGUACGA-3′), PI4K (5′-GCAAUGUGCUUCGCGAGAA-3′) and scrambled negative control (5′-GCAAGGGAAACCGUGUAAU-3′). Additional control siRNAs for SPCS1 were as follows: C911-#2 (5′-GCAAUAGUaccAUUUAUCU-3′), C911-#3 (5′-GAUGUUUCuccGAAUUAUU-3′) and C911-#4 (5′-GUUAUGGCgccAUUUGCUU-3′). Bases 9 through 11 of the siRNAs replaced with their complements were shown in lower cases.

Establishment of a stable cell line expressing the shRNA

Huh-7 cells were transfected with pSilencer-SPCS1, and drug-resistant clones were selected by treatment with hygromycin B (Wako, Tokyo, Japan) at a final concentration of 500 μg/ml for 4 weeks.

Virus

HCVtcp and HCVcc derived from JFH-1 having adaptive mutations in E2 (N417S), p7 (N765D), and NS2 (Q1012R) were generated as described previously [33]. The rAT strain of JEV [46] was used to generate virus stock.

Antibodies

Mouse monoclonal antibodies against actin (AC-15) and FLAG (M2) were obtained from Sigma-Aldrich (St. Louis, MO). Mouse

monoclonal antibodies against flavivirus group antigen (D1-4G2) were obtained from Millipore (Billerica, MA). Rabbit polyclonal antibodies against FLAG and V5 were obtained from Sigma-Aldrich. Rabbit polyclonal antibodies against SPCS1, claudin-1, PI4K and myc were obtained from Proteintech (Chicago, IL), Life Technologies (Carlsbad, CA), Cell Signaling (Danvers, MA) and Santa Cruz Biotechnology (Santa Cruz, CA), respectively. An anti-apoE goat polyclonal antibody was obtained from Millipore. Rabbit polyclonal antibodies against NS2 and NS3 were generated with synthetic peptides as antigens. Mouse monoclonal antibodies against HCV Core (2H9) and E2 (8D10-3) and rabbit polyclonal antibodies against NS5A and JEV are described elsewhere [47].

Titration

To determine the titers of HCVcc, Huh7.5.1 cells in 96-well plates were incubated with serially-diluted virus samples and then replaced with media containing 10% FBS and 0.8% carboxymethyl cellulose. Following incubation for 72 h, the monolayers were fixed and immunostained with the anti-NS5A antibody, followed by an Alexa Fluor 488-conjugated anti-rabbit secondary antibody (Invitrogen). Stained foci were counted and used to calculate the titers of focus-forming units (FFU)/ml. For intracellular infectivity of HCVcc, the pellets of infected cells were resuspended in culture medium and were lysed by four freeze-thaw cycles. After centrifugation for 5 min at 4,000 rpm, supernatants were collected and used for virus titration as above. For titration of JEV, Huh7.5.1 cells were incubated with serially-diluted virus samples and then replaced with media containing 10% FBS and 0.8% carboxymethyl cellulose. After a 24 h incubation, the monolayers were fixed and immunostained with a mouse monoclonal anti-flavivirus group antibody (D1-4G2), followed by an Alexa Fluor 488-conjugated anti-mouse secondary antibody (Invitrogen).

Immunoprecipitation

Transfected cells were washed with ice-cold PBS, and suspended in lysis buffer (20 mM Tris-HCl [pH 7.4] containing 135 mM NaCl, 1% TritonX-100, and 10% glycerol) supplemented with 50 mM NaF, 5 mM Na_3VO_4, and complete protease inhibitor cocktail, EDTA free (Roche). Cell lysates were sonicated for 10 min and then incubated for 30 min at 4°C, followed by centrifugation at 14,000× *g* for 10 min. The supernatants were immunoprecipitated with anti-Myc-agarose beads (sc-40, Santa Cruz Biotechnology) or anti-FLAG antibody in the presence of Dynabeads Protein G (Invitrogen). The immunocomplexes were precipitated with the beads by centrifugation at 800× *g* for 30 s, or by applying a magnetic field, and then were washed four times with the lysis buffer. The proteins binding to the beads were boiled with SDS sample buffer and then subjected to SDS–polyacrylamide gel electrophoresis (PAGE).

Immunoblotting

Transfected cells were washed with PBS and lysed with 50 mM Tris-HCl, pH 7.4, 300 mM NaCl, 1% Triton X-100. Lysates were then sonicated for 10 min and added to the same volume of SDS sample buffer. The protein samples were boiled for 10 min, separated by SDS-PAGE, and transferred to polyvinylidene difluoride membranes (Millipore). After blocking, the membranes were probed with the primary antibodies, followed by incubation with peroxidase-conjugated secondary antibody. Antigen-antibody complexes were visualized by an enhanced chemiluminescence detection system (Super Signal West Pico Chemiluminescent Substrate; PIERCE, Rockford, IL) according to the manufacturer's protocol and were detected by an LAS-3000 image analyzer system (Fujifilm, Tokyo, Japan).

Albumin measurement

To determine the human albumin level secreted from cells, culture supernatants were collected and passed through a 0.45-μm pore filter to remove cellular debris. The amounts of human albumin were quantified using a human albumin ELISA kit (Bethyl Laboratories, Montgomery, TX) according to the manufacturer's protocol.

Supporting Information

Figure S1 Effects of SPCS1-siRNAs and the C911 mismatch control siRNAs on the expression of SPCS1 and production of HCV. (A) Huh7.5.1 cells were transfected with either siRNAs targeted for SPCS1 (SPCS1-#2, -#3, and -#4), scrambled control siRNA (Scrambled) or C911 siRNA in which bases 9 through 11 of each SPCS1 siRNA were replaced with their complements (C911-#2, -#3, and -#4) at a final concentration of 15 nM, and were infected with HCVcc at a multiplicity of infection (MOI) of 0.05 at 24 h post-transfection. Expression levels of endogenous SPCS1 and actin in the cells were examined by immunoblotting using anti-SPCS1 and anti-actin antibodies at 3 days post-infection. (B) Infectious titers of HCVcc in the supernatant of the infected cells were determined at 3 days postinfection.
(TIF)

Figure S2 293T cells were transfected with E2 expression plasmid in the presence or absence of SPCS1-myc expression plasmid. The cell lysates of the transfected cells were immunoprecipitated with anti-myc antibody. The resulting precipitates and whole cell lysates used in IP were examined by immunoblotting using anti-E2 or anti-myc antibody. An empty plasmid was used as a negative control.
(TIF)

Figure S3 Interaction of HCV E2 with SPCS1 in mammalian cells. (A) 293T cells were transfected with indicated plasmids. 2 days posttransfection, cells were fixed and permeabilized with Triton X-100, then subjected to in situ PLA (Upper) or immunofluorescence staining (Lower) using anti-FLAG and anti-V5 antibodies. (B) Detection of the SPCS1-E2 interaction in transfected cells using the mKG system. 293T cells were transfected by indicated pair of mKG fusion constructs. Twenty-four hours after transfection, cell were fixed and stained with DAPI, and observed under a confocal microscope.
(TIF)

Acknowledgments

We are grateful to Francis V. Chisari (The Scripps Research Institute) for providing Huh7.5.1 cells, and Drs. C.K. Lim and T. Takasaki (National Institute of Infectious Diseases) for providing rabbit polyclonal anti-JEV antibodies. We thank M. Sasaki and T. Date for their technical assistance, and T. Mizoguchi for secretarial work. We also thank H. Hasegawa, T. Kato, T. Masaki, N. Watanabe, and A. Murayama for their helpful discussions.

Author Contributions

Conceived and designed the experiments: RS TS. Performed the experiments: RS MM. Analyzed the data: RS KW HA TS. Contributed reagents/materials/analysis tools: YM TW. Wrote the paper: RS TS.

References

1. Hoofnagle JH (2002) Course and outcome of hepatitis C. Hepatology 36: S21–29.
2. Suzuki T, Aizaki H, Murakami K, Shoji I, Wakita T (2007) Molecular biology of hepatitis C virus. J Gastroenterol 42: 411–423.
3. Appel N, Zayas M, Miller S, Krijnse-Locker J, Schaller T, et al. (2008) Essential role of domain III of nonstructural protein 5A for hepatitis C virus infectious particle assembly. PLoS Pathog 4: e1000035.
4. Dentzer TG, Lorenz IC, Evans MJ, Rice CM (2009) Determinants of the hepatitis C virus nonstructural protein 2 protease domain required for production of infectious virus. J Virol 83: 12702–12713.
5. Jirasko V, Montserret R, Appel N, Janvier A, Eustachi L, et al. (2008) Structural and functional characterization of nonstructural protein 2 for its role in hepatitis C virus assembly. J Biol Chem 283: 28546–28562.
6. Jones CT, Murray CL, Eastman DK, Tassello J, Rice CM (2007) Hepatitis C virus p7 and NS2 proteins are essential for production of infectious virus. J Virol 81: 8374–8383.
7. Ma Y, Yates J, Liang Y, Lemon SM, Yi M (2008) NS3 helicase domains involved in infectious intracellular hepatitis C virus particle assembly. J Virol 82: 7624–7639.
8. Masaki T, Suzuki R, Murakami K, Aizaki H, Ishii K, et al. (2008) Interaction of hepatitis C virus nonstructural protein 5A with core protein is critical for the production of infectious virus particles. J Virol 82: 7964–7976.
9. Tellinghuisen TL, Foss KL, Treadaway J (2008) Regulation of hepatitis C virion production via phosphorylation of the NS5A protein. PLoS Pathog 4: e1000032.
10. Phan T, Beran RK, Peters C, Lorenz IC, Lindenbach BD (2009) Hepatitis C virus NS2 protein contributes to virus particle assembly via opposing epistatic interactions with the E1–E2 glycoprotein and NS3-NS4A enzyme complexes. J Virol 83: 8379–8395.
11. Lorenz IC, Marcotrigiano J, Dentzer TG, Rice CM (2006) Structure of the catalytic domain of the hepatitis C virus NS2-3 protease. Nature 442: 831–835.
12. Lohmann V, Korner F, Koch J, Herian U, Theilmann L, et al. (1999) Replication of subgenomic hepatitis C virus RNAs in a hepatoma cell line. Science 285: 110–113.
13. Kato T, Choi Y, Elmowalid G, Sapp RK, Barth H, et al. (2008) Hepatitis C virus JFH-1 strain infection in chimpanzees is associated with low pathogenicity and emergence of an adaptive mutation. Hepatology 48: 732–740.
14. Scheel TK, Gottwein JM, Jensen TB, Prentoe JC, Hoegh AM, et al. (2008) Development of JFH1-based cell culture systems for hepatitis C virus genotype 4a and evidence for cross-genotype neutralization. Proc Natl Acad Sci U S A 105: 997–1002.
15. Jensen TB, Gottwein JM, Scheel TK, Hoegh AM, Eugen-Olsen J, et al. (2008) Highly efficient JFH1-based cell-culture system for hepatitis C virus genotype 5a: failure of homologous neutralizing-antibody treatment to control infection. J Infect Dis 198: 1756–1765.
16. Yi M, Ma Y, Yates J, Lemon SM (2007) Compensatory mutations in E1, p7, NS2, and NS3 enhance yields of cell culture-infectious intergenotypic chimeric hepatitis C virus. J Virol 81: 629–638.
17. Russell RS, Meunier JC, Takikawa S, Faulk K, Engle RE, et al. (2008) Advantages of a single-cycle production assay to study cell culture-adaptive mutations of hepatitis C virus. Proc Natl Acad Sci U S A 105: 4370–4375.
18. Popescu CI, Callens N, Trinel D, Roingeard P, Moradpour D, et al. (2011) NS2 protein of hepatitis C virus interacts with structural and non-structural proteins towards virus assembly. PLoS Pathog 7: e1001278.
19. Ma Y, Anantpadma M, Timpe JM, Shanmugam S, Singh SM, et al. (2011) Hepatitis C virus NS2 protein serves as a scaffold for virus assembly by interacting with both structural and nonstructural proteins. J Virol 85: 86–97.
20. Stapleford KA, Lindenbach BD (2011) Hepatitis C virus NS2 coordinates virus particle assembly through physical interactions with the E1–E2 glycoprotein and NS3-NS4A enzyme complexes. J Virol 85: 1706–1717.
21. Jirasko V, Montserret R, Lee JY, Gouttenoire J, Moradpour D, et al. (2010) Structural and functional studies of nonstructural protein 2 of the hepatitis C virus reveal its key role as organizer of virion assembly. PLoS Pathog 6: e1001233.
22. Yi M, Ma Y, Yates J, Lemon SM (2009) Trans-complementation of an NS2 defect in a late step in hepatitis C virus (HCV) particle assembly and maturation. PLoS Pathog 5: e1000403.
23. Counihan NA, Rawlinson SM, Lindenbach BD (2011) Trafficking of hepatitis C virus core protein during virus particle assembly. PLoS Pathog 7: e1002302.
24. Kiiver K, Merits A, Ustav M, Zusinaite E (2006) Complex formation between hepatitis C virus NS2 and NS3 proteins. Virus Res 117: 264–272.
25. Selby MJ, Glazer E, Masiarz F, Houghton M (1994) Complex processing and protein:protein interactions in the E2:NS2 region of HCV. Virology 204: 114–122.
26. Johnsson N, Varshavsky A (1994) Split ubiquitin as a sensor of protein interactions in vivo. Proc Natl Acad Sci U S A 91: 10340–10344.
27. Evans E, A., Gilmore R, Blobel G (1986) Purification of microsomal signal peptidase as a complex. Proc Natl Acad Sci U S A 83: 581–585.
28. Fang H, Panzner S, Mullins C, Hartmann E, Green N (1996) The homologue of mammalian SPC12 is important for efficient signal peptidase activity in Saccharomyces cerevisiae. J Biol Chem 271: 16460–16465.
29. Wakita T, Pietschmann T, Kato T, Date T, Miyamoto M, et al. (2005) Production of infectious hepatitis C virus in tissue culture from a cloned viral genome. Nat Med 11: 791–796.
30. Söderberg O, Gullberg M, Jarvius M, Ridderstrale K, Leuchowius KJ, et al. (2006) Direct observation of individual endogenous protein complexes in situ by proximity ligation. Nat Methods 3: 995–1000.
31. Kerppola TK (2006) Complementary methods for studies of protein interactions in living cells. Nat Methods 3: 969–971.
32. Buehler E, Chen YC, Martin S (2012) C911: A bench-level control for sequence specific siRNA off-target effects. PLoS One 7: e51942.
33. Suzuki R, Saito K, Kato T, Shirakura M, Akazawa D, et al. (2012) Trans-complemented hepatitis C virus particles as a versatile tool for study of virus assembly and infection. Virology 432: 29–38.
34. Chang KS, Jiang J, Cai Z, Luo G (2007) Human apolipoprotein E is required for infectivity and production of hepatitis C virus in cell culture. J Virol 81: 13783–13793.
35. Owen DM, Huang H, Ye J, Gale M, Jr. (2009) Apolipoprotein E on hepatitis C virion facilitates infection through interaction with low-density lipoprotein receptor. Virology 394: 99–108.
36. Akazawa D, Date T, Morikawa K, Murayama A, Miyamoto M, et al. (2007) CD81 expression is important for the permissiveness of Huh7 cell clones for heterogeneous hepatitis C virus infection. J Virol 81: 5036–5045.
37. Erdtmann L, Franck N, Lerat H, Le Seyec J, Gilot D, et al. (2003) The hepatitis C virus NS2 protein is an inhibitor of CIDE-B-induced apoptosis. J Biol Chem 278: 18256–18264.
38. de Chassey B, Navratil V, Tafforeau L, Hiet MS, Aublin-Gex A, et al. (2008) Hepatitis C virus infection protein network. Mol Syst Biol 4: 230.
39. Stagljar I, Korostensky C, Johnsson N, te Heesen S (1998) A genetic system based on split-ubiquitin for the analysis of interactions between membrane proteins in vivo. Proc Natl Acad Sci U S A 95: 5187–5192.
40. Kalies KU, Hartmann E (1996) Membrane topology of the 12- and the 25-kDa subunits of the mammalian signal peptidase complex. J Biol Chem 271: 3925–3929.
41. Mullins C, Meyer HA, Hartmann E, Green N, Fang H (1996) Structurally related Spc1p and Spc2p of yeast signal peptidase complex are functionally distinct. J Biol Chem 271: 29094–29099.
42. Li Q, Brass AL, Ng A, Hu Z, Xavier RJ, et al. (2009) A genome-wide genetic screen for host factors required for hepatitis C virus propagation. Proc Natl Acad Sci U S A 106: 16410–16415.
43. Zhong J, Gastaminza P, Cheng G, Kapadia S, Kato T, et al. (2005) Robust hepatitis C virus infection in vitro. Proc Natl Acad Sci U S A 102: 9294–9299.
44. Masaki T, Suzuki R, Saeed M, Mori K, Matsuda M, et al. (2010) Production of infectious hepatitis C virus by using RNA polymerase I-mediated transcription. J Virol 84: 5824–5835.
45. Suzuki R, Sakamoto S, Tsutsumi T, Rikimaru A, Tanaka K, et al. (2005) Molecular determinants for subcellular localization of hepatitis C virus core protein. J Virol 79: 1271–1281.
46. Zhao Z, Date T, Li Y, Kato T, Miyamoto M, et al. (2005) Characterization of the E-138 (Glu/Lys) mutation in Japanese encephalitis virus by using a stable, full-length, infectious cDNA clone. J Gen Virol 86: 2209–2220.
47. Saeed M, Suzuki R, Watanabe N, Masaki T, Tomonaga M, et al. (2011) Role of the endoplasmic reticulum-associated degradation (ERAD) pathway in degradation of hepatitis C virus envelope proteins and production of virus particles. J Biol Chem 286: 37264–37273.

SCIENTIFIC REPORTS

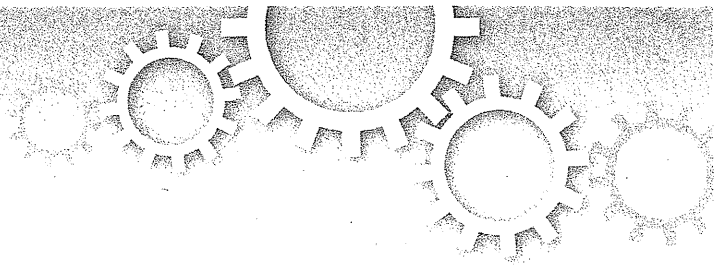

OPEN

SUBJECT AREAS:
MECHANISMS OF DISEASE
HEPATITIS C
LIVER FIBROSIS
TRANSFORMING GROWTH FACTOR BETA

Received
25 July 2013

Accepted
31 October 2013

Published
22 November 2013

Correspondence and requests for materials should be addressed to S.K. (skojima@riken.jp)

HCV NS3 protease enhances liver fibrosis via binding to and activating TGF-β type I receptor

Kotaro Sakata[1,2,3], Mitsuko Hara[1], Takaho Terada[4,5], Noriyuki Watanabe[6], Daisuke Takaya[4,7], So-ichi Yaguchi[8], Takehisa Matsumoto[4,7], Tomokazu Matsuura[9], Mikako Shirouzu[4,7], Shigeyuki Yokoyama[4,5], Tokio Yamaguchi[10], Keiji Miyazawa[8], Hideki Aizaki[6], Tetsuro Suzuki[11], Takaji Wakita[6], Masaya Imoto[2] & Soichi Kojima[1]

[1]Micro-signaling Regulation Technology Unit, RIKEN Center for Life Science Technologies, Saitama 351-0198, Japan, [2]Department of Biosciences and Informatics, Faculty of Science and Technology, Keio University, Kanagawa 223-8522, Japan, [3]Drug Discovery Laboratory, Wakunaga Pharmaceutical Co., Ltd., Hiroshima 739-1195, Japan, [4]RIKEN Systems and Structural Biology Center, Kanagawa 230-0045, Japan, [5]RIKEN Structural Biology Laboratory, Kanagawa 230-0045, Japan, [6]Department of Virology II, National Institute of Infectious Diseases, Tokyo 162-8640, Japan, [7]Division of Structural and Synthetic Biology, RIKEN Center for Life Science Technologies, Kanagawa 230-0045, Japan, [8]Department of Biochemistry, Interdisciplinary Graduate School of Medicine and Engineering, University of Yamanashi, Yamanashi 409-3898, Japan, [9]Department of Laboratory Medicine, the Jikei University School of Medicine, Tokyo 105-8461, Japan, [10]RIKEN Program for Drug Discovery and Medical Technology Platforms, Saitama 351-0198, Japan, [11]Department of Infectious Diseases, Hamamatsu University School of Medicine, Shizuoka 431-3192, Japan.

Viruses sometimes mimic host proteins and hijack the host cell machinery. Hepatitis C virus (HCV) causes liver fibrosis, a process largely mediated by the overexpression of transforming growth factor (TGF)-β and collagen, although the precise underlying mechanism is unknown. Here, we report that HCV non-structural protein 3 (NS3) protease affects the antigenicity and bioactivity of TGF-β2 in $(CAGA)_9$-Luc CCL64 cells and in human hepatic cell lines via binding to TGF-β type I receptor (TβRI). Tumor necrosis factor (TNF)-α facilitates this mechanism by increasing the colocalization of TβRI with NS3 protease on the surface of HCV-infected cells. An anti-NS3 antibody against computationally predicted binding sites for TβRI blocked the TGF-β mimetic activities of NS3 *in vitro* and attenuated liver fibrosis in HCV-infected chimeric mice. These data suggest that HCV NS3 protease mimics TGF-β2 and functions, at least in part, via directly binding to and activating TβRI, thereby enhancing liver fibrosis.

Viruses sometimes take over the host cell machinery by mimicking host cell proteins. This strategy infers survival, infection, and replication advantages to the virus[1,2], which may thereby contribute to the development of human disease.

Chronic hepatitis C virus (HCV) infection is one of the major causes of liver fibrosis, cirrhosis, and hepatocellular carcinoma[3,4]. However, the molecular mechanism by which HCV induces liver fibrosis is not fully understood. An estimated 130–170 million people worldwide are infected with HCV[5]. HCV, classified in the genus *Hepacivirus* of the family *Flaviviridae*, is a positive-strand RNA virus with an approximately 9.6-kb viral genome encoding structural (core, E1, and E2) and non-structural proteins (p7, NS2, NS3, NS4A, NS4B, NS5A, and NS5B)[6]. Of these proteins, NS3 is a member of the serine protease family that cleaves the HCV polyprotein to generate mature viral proteins that are required for viral replication[7].

Liver fibrosis, a common feature of chronic liver diseases, is caused by the excessive accumulation of extracellular matrix (ECM) proteins, including collagen. Transforming growth factor (TGF)-β, the most potent fibrogenic cytokine, is produced in its high molecular weight latent form and partly activated through the proteolytic cleavage of its propeptide region, termed latency associated protein (LAP), by serine proteases, plasmin, and plasma kallikrein[8,9]. The resultant active TGF-β signals via TGF-β type I (TβRI) and type II receptors (TβRII), inducing the phosphorylation of Smad2/3, which then binds to Smad4 and forms a complex that enters the cell nucleus. This complex acts as a transcription factor that controls the expression of target genes, including collagen and TGF-β itself, by binding to the DNA elements containing the minimal Smad-binding element, CAGA-box[10].

Because the LAPs of TGF-β2 and -β3 have sequences that share partially homology with the NS3 cleavage site between NS3 and NS4A of HCV[7], we speculated that NS3 might activate TGF-β2 and/or TGF-β3 via the proteolytic cleavage of their LAP portions. We found, however, that NS3 protease DID NOT directly activate latent TGF-β2/3. Instead, it mimicked TGF-β2 and induced TGF-β signaling by binding and activating TβRI, leading to the induction of fibrogenic genes. This pathway was enhanced in the presence of an inflammatory cytokine, tumor necrosis factor (TNF)-α, as TNF-α increased the expression of TβRI. Furthermore, we found that NS3 colocalized with TβRI on the surface of an HCV-infected hepatoma cell line, and we observed direct binding between recombinant NS3 and TβRI. These phenomena were reproduced in chimeric mice transplanted with human hepatocytes that had been infected with HCV. These data suggest a novel mechanism by which HCV induces liver fibrosis.

Results

HCV NS3 protease exerted TGF-β mimetic activity via TβRI. To confirm whether HCV NS3 protease might induce the activation of latent TGF-β2, bacterially expressed recombinant NS3 (Supplementary Fig. S1) was incubated with conditioned medium obtained from HEK293T cells transiently overexpressing latent TGF-β2, and the concentration of active TGF-β2 in the reaction mixtures were measured by ELISA. Although the addition of NS3 increased active TGF-β2 concentrations in a dose-dependent manner, these increases were not time-dependent (Supplementary Fig. S2). Instead, we found that NS3 protease itself reacted with TGF-β2 in a dose-dependent manner, as determined by ELISA (Fig. 1A). Next, to assess whether NS3 could induce the bioactivity of TGF-β via TβRI, and whether its activity was dependent on protease activity, we performed a luciferase reporter assay with the TGF-β-responsive $(CAGA)_9$-Luc reporter in CCL64 cells. NS3 demonstrated TGF-β mimetic activity, which was alleviated in the presence of TβRI kinase inhibitors (SB-431542 and LY-364947) in a dose-dependent manner (Fig. 1B). In contrast, an NS3 protease inhibitor, VX-950 (telaprevir), did not affect luciferase activity (Fig. 1B). An unrelated protein with almost the same molecular weight as NS3, HLA class II histocompatibility antigen, DM α chain (HLA-DMA), as well as a carrier-free, tag-control sample, did not exert TGF-β mimetic activity, thus demonstrating the specificity of NS3 (Supplementary Fig. S3). Additionally, an anti-TGF-β2 antibody that detected NS3 in the TGF-β2 ELISA did not inhibit luciferase activity (Supplementary Fig. S4).

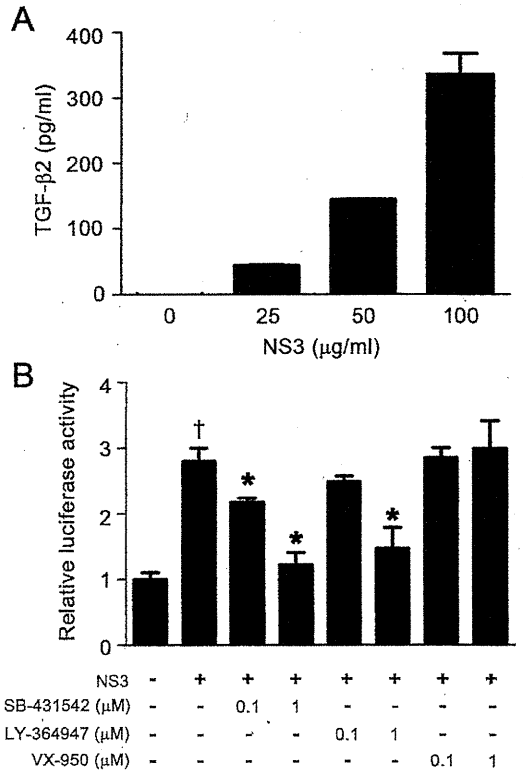

Figure 1 | HCV NS3 protease exerted TGF-β mimetic activity via the type I receptor. (A) TGF-β2 antigenicity of NS3. The indicated concentrations of recombinant NS3 protease were used in the TGF-β2 ELISA assays. (B) TGF-β mimetic activity of NS3 and its suppression by TβRI kinase inhibitors. $(CAGA)_9$-Luc CCL64 cells were stimulated with 100 μg/ml of recombinant NS3 protease for 24 hours, with or without the indicated concentration of TβRI kinase inhibitor or the NS3 protease inhibitor VX-950 (telaprevir). After 24 hours, the cells were harvested and luciferase activity measured. †$p < 0.05$ compared with untreated control cells, *$p < 0.05$ compared with NS3-treated cells without any inhibitors. The data are shown as the mean ± SD (n = 3), and representative results from three independent experiments with similar results are shown.

NS3 stimulated collagen production in hepatic cells, which was augmented by TNF-α. We examined the effect of NS3 on the expression of TGF-β1 and collagen α1 (I) in the human hepatic stellate cell line LX-2. Treatment with NS3 for 12 hours significantly increased both TGF-β1 (1.6-fold) and collagen α1 (I) (1.4-fold) expression in these cells (Fig. 2A). On the contrary, NS3 did not affect the expression of these genes in the normal hepatic cell line Hc. The pretreatment of the cells with tumor necrosis factor-α (TNF-α) enhanced increased TGF-β1 and collagen α1 (I) expression mediated by NS3 and was also accompanied by an increase in TGF-β receptor expression (Fig. 2B). Further increases in TβRI expression were not observed by combination treatment with TNF-α, suggesting that TNF-α increased TβRI expression, which may have enhanced the TGF-β mimetic activity of NS3 in these cells. Furthermore, Smad3 phosphorylation was also induced by NS3 in Hc cells that had been pretreated with TNF-α (Fig. 2D). A similar cooperativity between TNF-α and NS3 protease was not observed in LX-2 cells (Fig. 2C).

Interaction between NS3 and TβRI on the surface of HCV-infected HCC cells. NS3 was immunostained on the surface of HCV-infected Huh-7.5.1 cells both with and without permeabilization. In contrast, an ER marker, calnexin, was only positive after the permeabilization of the cells (Fig. 3A). To examine whether NS3 that was localized to the surface of HCV-infected Huh-7.5.1 cells interacted with TβRI, we performed co-immunostaining (Fig. 3B) and in situ proximity ligation assay (PLA) (Fig. 3C) using antibodies against NS3 and TβRI. Both results showed that NS3 was colocalized and formed a complex with TβRI on the cell surface. Because LX-2 cells (hepatic stellate cells) are not infected with HCV, the data were not recorded. We also co-cultured Huh-7.5.1 infected with HCV and LX-2 cells and examined them using *in situ* PLA. However, the interaction between NS3 protease and TβRI was not observed on the surface of LX-2 cells. Furthermore, we performed co-immunoprecipitation assays using recombinant NS3 and the extracellular domain of TβRI and TβRII. As shown in Figure 3D, FLAG-tagged NS3 bound to TβRI and TβRII, whereas FLAG-tag alone failed to interact with TGF-β receptors (Fig. 3D and Supplementary Fig. S5).

Docking simulation using the Katchalski-Katzir algorithm predicted that NS3 interacts with TβRI at three sites, T22-S42, T76-P96, and G120-S139, in NS3 and F55-M70, I72-V85, and C86-Y99 in TβRI, respectively (Fig. 3E, Table 1, and Supplementary Fig. S6). The predicted binding site peptides, particularly the peptide derived from site 3, completely blocked the interaction between NS3 and

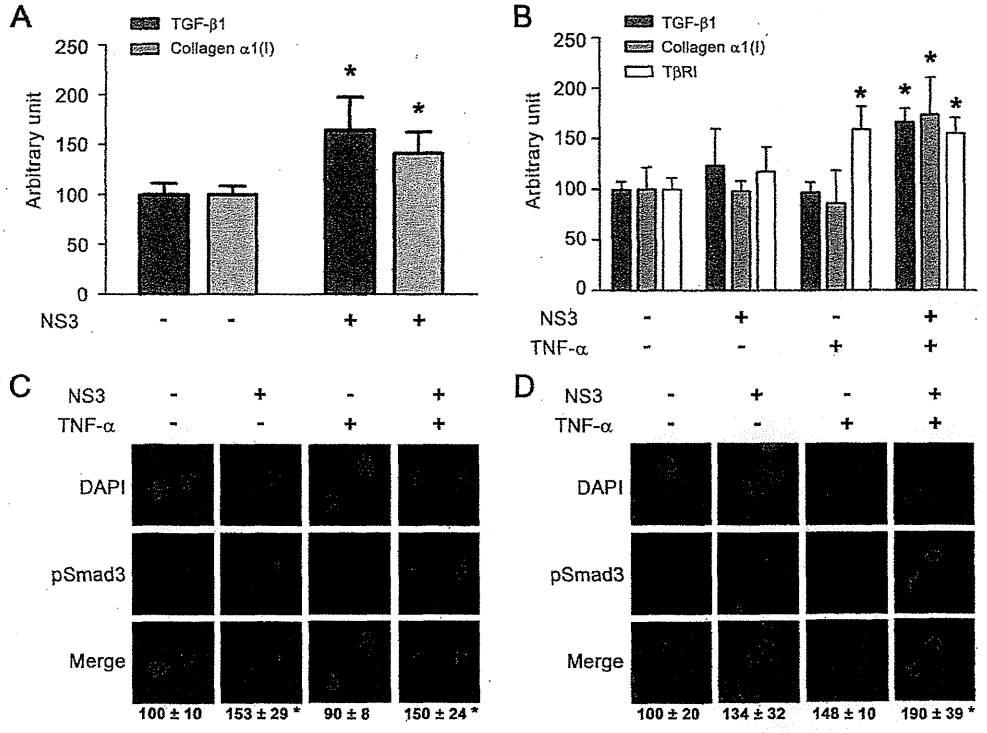

Figure 2 | Cooperativity between NS3 and TNF-α in the stimulation of TGF-β1, collagen α1 (I), and TβRI expression. (A) Effect on TGF-β1 and collagen α1(I) mRNA expression in LX-2 cells. The cells were stimulated with 50 μg/ml of NS3 for 12 hours. Total cellular RNA was isolated and reverse transcribed to cDNA, and real-time PCR was performed as described in the Methods section. $*p < 0.05$ compared with untreated control cells. (B) Effect of pretreatment with TNF-α on the stimulation of expression of TGF-β1, collagen α1(I), and TβRI by NS3 protease in HC cells. Following the pretreatment of the cells with 20 ng/ml TNF-α for 12 hours, they were stimulated with 25 μg/ml NS3 for 12 hours, and mRNA expression was measured as described above. $*p < 0.05$ compared with untreated cells. The data are shown as the mean ± SD (n = 3). (C and D) The effect of pretreatment with TNF-α on the stimulation of phosphorylation of Smad3 by NS3 protease in LX-2 cells (C) and Hc cells (D). After the cells were treated with 20 ng/ml TNF-α for 12 hours and 25 μg/ml NS3 for another 12 hours, they were fixed, and immunofluorescent staining was performed as described in the Methods section. The experiments were performed in duplicate. The relative fluorescence intensities of phospho-Smad3 (% of untreated control cells) in 4 randomly selected fields from each dish were calculated with ZEN software and are shown as the mean ± SD. The results are representative of three independent experiments with similar results.

TβRI in the immunoprecipitation experiment (Supplementary Fig. S7A). Antibodies produced to these predicted binding sites within both NS3 and TβRI decreased the TGF-β mimetic activity of NS3 in $(CAGA)_9$-Luc CCL64 cells (Fig. 3F–H). Furthermore, the anti-NS3 antibody inhibited HCV-induced Smad3 phosphorylation (Supplementary Fig. S7B).

Anti-NS3 antibody prevented liver fibrosis in HCV-infected chimeric mice. To test our hypothesis that NS3 exerts TGF-β mimetic activity, thereby causing liver fibrosis, we examined whether the anti-NS3 antibody could prevent liver fibrosis in HCV-infected human hepatocyte-transplanted chimeric mice. The anti-NS3 antibody significantly prevented hepatic collagen accumulation in the mice (Fig. 4A) and decreased the mRNA expression of both TGF-β1 and collagen α1 (I) (Fig. 4B and 4C). There was no significant change in the serum levels of human albumin and HCV RNA during treatment with the anti-NS3 antibody (Supplementary Fig. S8A and S8B).

Discussion

Several groups have studied the molecular mechanisms by which HCV induces liver fibrosis and have reported the following: (i) HCV core protein activates the TGF-β1 promoter via the MAPK pathway in core protein-expressing human hepatocellular carcinoma HepG2 cells[11]; (ii) recombinant core protein upregulates the expression of fibrogenic genes in the human hepatic stellate cell line LX-2 via the toll-like receptor 2 [12] and the obese receptor[13]; and (iii) NS3 protease induces TGF-β1 production in NS3-over-expressing human hepatoma Huh-7 cells[14]. Our data show that NS3 protease mimics TGF-β2 and directly exerts its activity, at least in part, via binding to and activating TβRI, thereby enhancing liver fibrosis. The following experiments should be carried out in the future: effect of NS3 on TβRI phosphorylation, the expression of TGF-β2, TGF-β3, and other TGF-β responsive genes, such as plasminogen activator inhibitor-1, a tissue inhibitor of metalloproteinase-1, and α-smooth muscle actin, to further validate the TGF-β mimetic activity of NS3.

HCV NS3 is a chimera of a helicase and serine protease, which cleaves not only the junction between NS3-4A, NS4A-4B, NS4B-5A, and NS5A-5B for viral polyprotein processing, which is essential to the viral lifecycle, but also the toll-interleukin-1 receptor domain-containing, adaptor-inducing beta interferon, and mitochondrial antiviral signaling protein, which results in the disruption of innate immune responses[7,15]. An NS3 protease inhibitor, telaprevir, which was approved by the FDA in 2011, has been used in triple combination therapy with the current standard treatment of PEGylated interferon and ribavirin[16]. Telaprevir did not inhibit TGF-β mimetic activity in a $(CAGA)_9$-Luc reporter gene assay (Fig. 1C), suggesting that the TGF-β mimetic activity of NS3 is independent of its protease activity.

Much interest has centered on the fact that extraordinarily high concentrations of NS3 protease, up to 100 μg/ml, could exist in

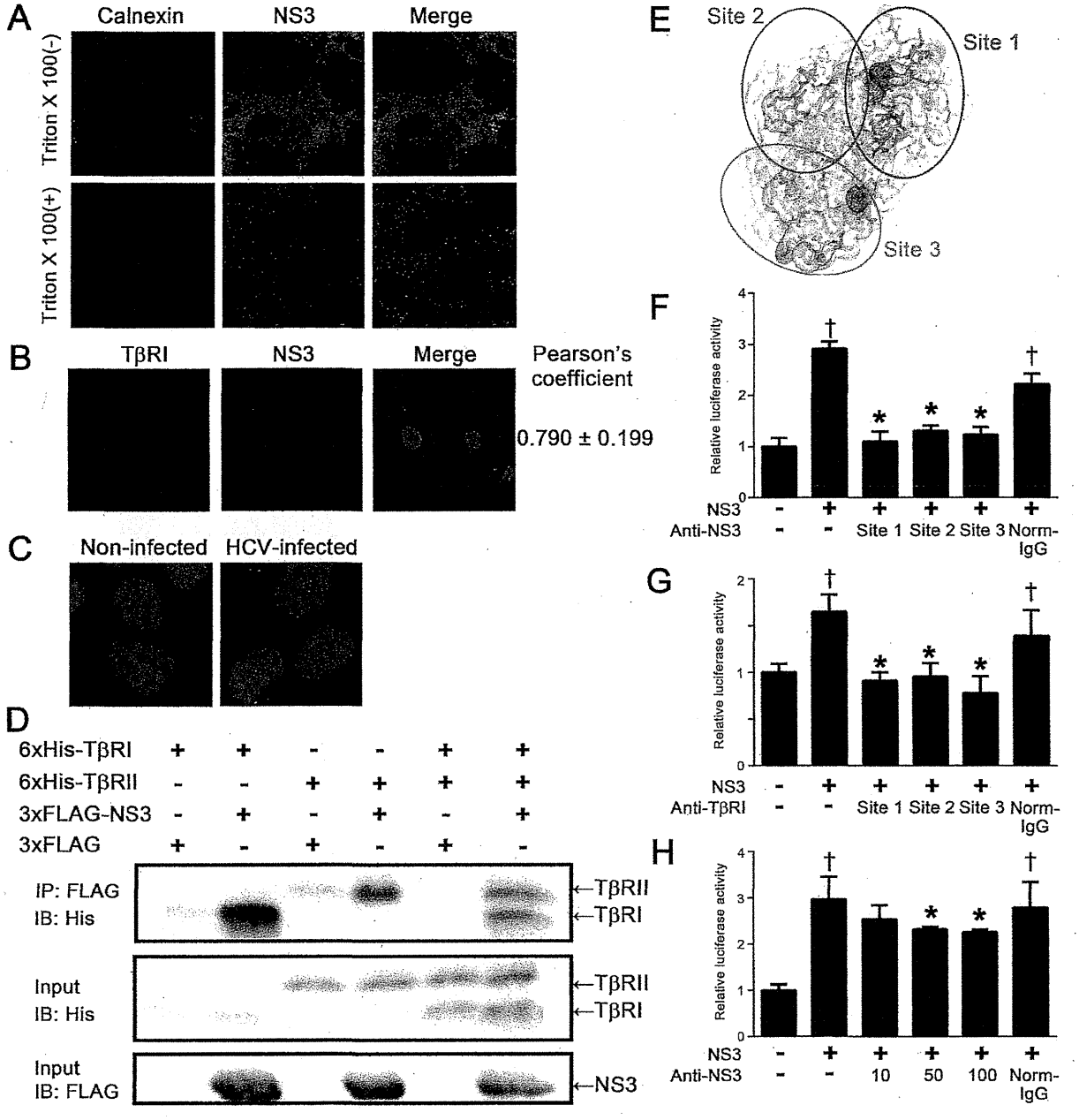

Figure 3 | NS3 protease colocalized and directly interacted with TβRI on the surface of HCV-infected cells. (A) The detection of NS3 protease on the surface of HCV-infected Huh-7.5.1 cells. The cells were fixed, followed ± by permeabilization with Triton-X 100, and then stained with DAPI, anti-NS3 antibody, and anti-calnexin antibody. (B) The colocalization of NS3 protease with TβRI in HCV-infected Huh7.5.1 cells. The cells were fixed and stained with DAPI, anti-NS3 antibody, and anti-TβRI antibody, as described in the Methods section. Pearson's colocalization coefficient values were obtained from 4 randomly selected fields using the ZEN software. The results are shown as the mean ± SD and are representative of three independent experiments with similar results. (C) The detection of NS3-TβRI proximity by in situ PLA in HCV-infected Huh-7.5.1 cells. The red dots indicate interactions between NS3 protease and TβRI, and the nuclei were identified by DAPI staining. (D) The physical interaction of NS3protease with TβRI and TβRII. FLAG-tagged NS3protease was incubated with 6xHis-tagged TβRI and/or TβRII and immunoprecipitated. The coprecipitated proteins were visualized by immunoblotting using anti-His antibody. The gels were run under the same experimental conditions. Cropped blots are shown (full-length blots are presented in Supplementary Fig. S5). (E) The structural overview of the NS3protease. The indicated colored amino acids (site 1, red; site 2, magenta; and site 3, cyan) show the important residues within the putative binding sites to TβRI, and the sequences are presented in Table 1. TGF-β mimetic activity of NS3 was inhibited in the presence of either anti-NS3 polyclonal antibodies against the predicted binding sites of TβRI (F), or anti-TβRI polyclonal antibodies against predicted binding sites of NS3 (G), and anti-NS3 monoclonal antibody against predicted binding site 3 of TβRI (H). Luciferase activities in $(CAGA)_9$-Luc CCL64 cells were measured as before. Normal mouse IgG (Norm-IgG) was used as a negative control. The data are shown as the mean ± SD. †$p < 0.05$ compared with untreated control cells, *$p < 0.05$ compared with NS3-treated cells without any antibodies. Representative results from three independent experiments with similar results are shown.

Table 1 | The amino acid sequences of predicted binding sites between NS3 protease and TβRI

	NS3 protease	TβRI
Site 1	TGRDKNQVEGEVQVVSTATQS	FVSVTETTDKVIHNSM
Site 2	TNVDQDLVGWPAPPGARSLTP	IAEIDLIPRDRPFV
Site 3	GDNRGSLLSPRPVSYLKGSS	CAPSSKTGSVTITY

The underlined letters denote the putative contact residues.

proximity to a TGF-β receptor. This line of inquiry led us to identify the cooperativity between NS3 and TNF-α, although the cooperative effect was maximal at one fourth this concentration of NS3. Serum levels of TNF-α in chronic hepatitis C patients are known to be significantly higher than those in healthy subjects[17,18]. We showed that TNF-α increased the susceptibility of cells to NS3 by enhancing the expression of TβRI, thereby further increasing the levels of profibrogenic genes (Fig. 2B). Various hepatic cell lines expressed different levels of TβRI, and there appeared to be a threshold in the level of TβRI that enabled cells to produce collagen mRNA upon stimulation with NS3. In particular, Hc cells expressed levels of TβRI below this predicted threshold (Supplementary Fig. S9). Consistent with our findings, carbon tetrachloride has recently been reported to induce acute liver injury, specifically significant liver fibrosis with inflammation, in transgenic mice expressing the full-length HCV polyprotein[19].

We documented the colocalization of NS3 and TβRI on the cell surface of HCV JFH-1-infected Huh-7.5.1 cells (Fig. 3). The results of co-immunoprecipitation and in situ PLA studies supported this conclusion. In future studies, we intend to use mutagenesis experiments of the predicted binding site and competition assays using NS3 and TGF-β in $(CAGA)_9$-Luc CCL64 cells to determine the mechanism of NS3 and TβRI binding. However, at present, how NS3 is released to the extracellular milieu remains to be elucidated. One possibility is that NS3 leaks passively from injured hepatocytes, as is the case for alanine aminotransferase and aspartate aminotransferase. Another possibility is that NS3 is secreted from HCV-infected cells via the Golgi complex. A recent report showed that nonstructural protein (NS) 1 of the dengue virus (DENV) and West Nile virus (WNV) is secreted from DENV- and WNV-infected cells through the Golgi complex following expression in association with the endoplasmic reticulum. Like HCV, these viruses are also members of the family *Flaviviridae*[20].

Zhang et al.[21] identified antibodies against NS3 in the serum of chronic hepatitis C patients and suggested that extracellular NS3 may be present in such cases. However, it remains unclear whether the concentration of HCV NS3 is as high as in our in vitro experiments. Although DENV NS1 has been reportedly detected at high levels (up to 50 μg/ml) in the serum of DENV-infected patients[22], further study is warranted to determine the serum or tissue NS3 concentrations in patients with chronic hepatitis C.

In this study, we generated polyclonal and monoclonal anti-NS3 antibodies that block the NS3-TβRI interaction. All anti-NS3 and anti-TβRI polyclonal antibodies generated against the predicted binding sites almost completely blocked TGF-β mimetic activity. This finding was likely due to steric hindrance by these antibodies or a requirement of binding at all three sites for signal transduction by NS3. The monoclonal antibody is a powerful tool that can be used to explore our working hypothesis that NS3 enhances liver fibrosis via the TGF-β receptor *in vivo*. We showed that the anti-NS3 monoclonal antibody generated against a predicted binding site to TβRI ameliorated liver fibrosis in HCV-infected human hepatocyte transplanted chimeric mice (Fig. 4A–C). The control of fibrosis after the eradication of the virus determines the prognosis, including the likelihood of progression to tumorigenesis. Therefore, the NS3 antibody

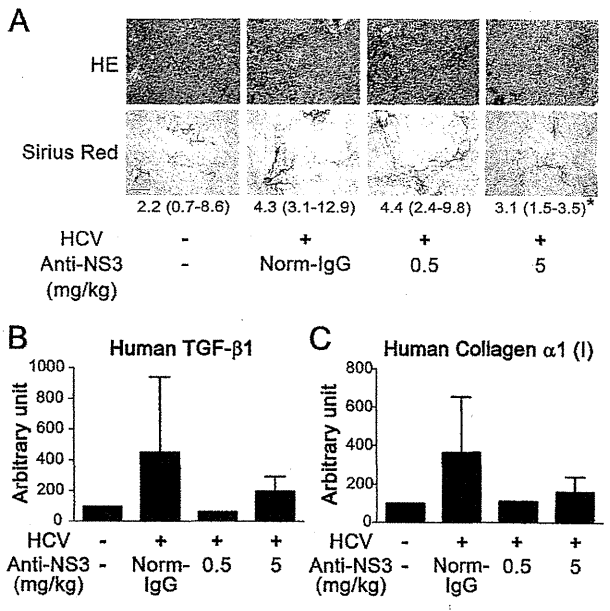

Figure 4 | Anti-NS3 antibody attenuated liver fibrosis in the HCV-infected chimeric mice. (A) Staining of liver sections. Paraffin sections were prepared from the livers of HCV-infected chimeric mice 16 weeks after HCV inoculation, and stained with hematoxylin and eosin (upper panels) and Sirius Red (lower panels). An anti-NS3 antibody was administered at the indicated doses, and normal mouse IgG (Norm-IgG) was administered at a dose of 5 mg/kg. For each group, the median ratios in Sirius Red positive/total area (%) from 6 randomly selected fields are shown, with the range in parentheses. $*p < 0.05$ compared with HCV-infected mice without anti-NS3 antibody. Scale bar = 100 μm. The representative result from 6 randomly selected fields is shown. (B) and (C) Hepatic mRNA expression in HCV-infected chimeric mice. Total RNA was isolated from the livers of these mice and reverse transcribed to cDNA, and real-time PCR was performed as described in the Methods section to quantitate the expression of human TGF-β1 expression (B) and human collagen α1 (I) (C). The data are shown as the mean ± SD, and representative results from two independent experiments with similar results are shown.

against the TβRI binding site might have a clinical benefit in HCV patients with cirrhosis after combination therapy.

In conclusion, we demonstrated for the first time that HCV NS3 protease serves as a novel TGF-β receptor ligand and enhances liver fibrosis. This phenomenon might be beneficial to the virus, as TGF-β signals suppress host immunity. Our results provide elucidation regarding the molecular mechanism by which HCV induces liver fibrosis.

Methods

Materials. SB-431542 and LY-364947 were purchased from Sigma-Aldrich (St. Louis, MO). Recombinant human TNF-α was purchased from R&D systems, Inc. (Minneapolis, MN). Anti-NS3 antibody and anti-calnexin antibody were purchased from Abcam (Cambridge, UK). Anti-TβRI antibody and anti-phospho-Smad3 antibody were purchased from Santa Cruz Biotechnology (Santa Cruz, CA) and Immuno-Biological Laboratories (Gunma, Japan), respectively. Anti-Flag M2 antibody and anti-His antibody were purchased from Sigma (St. Louis, MO). Anti-NS3 antibodies and anti-TβRI antibodies against predicted binding sites were provided by the BioMatrix Research Institute (Chiba, Japan).

Cell culture. $(CAGA)_9$-Luc CCL64 cells were kindly provided by Prof. Hideaki Kakeya (Kyoto University, Kyoto, Japan), the hepatic stellate cell line LX-2 was kindly provided by Prof. Norifumi Kawada (Osaka City University, Osaka, Japan), and the human hepatoma cell line Huh-7.5.1 were maintained in Dulbecco's modified Eagle's medium (DMEM) supplemented with 10% fetal bovine serum, penicillin, and streptomycin. HC cells, a normal human hepatocyte cell line purchased from Cell Systems (Kirkland, WA), were cultured in CS-C complete medium (Kirkland, WA).

Protein preparation. The N-terminal histidine or 3xFLAG-tagged NS3 protease, and the extracellular domain of human TβRI and TβRII were expressed in *Escherichia coli* by isopropyl-β-thiogalactopyranoside induction. The protein was purified by affinity chromatography in a HisTrap HP column (GE Healthcare, Waukesha, WI). Detailed procedures are in the Supplementary information.

Enzyme-linked immunosorbent assay (ELISA). TGF-β2 ELISA was performed using a TGF-β2 Emax® Immune Assay System ELISA kit (Promega, Madison, WI) according to the manufacturer's instructions.

Luciferase assay. The mink lung epithelial cell line CCL64, which stably expressed $(CAGA)_9$-MLP-luciferase and contained nine copies of a Smad-binding CAGA box element upstream of a minimal adenovirus major late promoter (2×10^4 cells/well)[23], was seeded into 96-well plates. The next day, the medium was replaced with fresh medium containing 0.1% bovine serum albumin, and the cells were cultured for an additional 24 hours. The cells were extracted with lysis buffer, and luciferase activity was measured by a Luciferase Assay System (Promega, Madison, WI) according to the manufacturer's instructions.

Real-time RT-PCR. The isolation of total RNA and real-time RT-PCR were performed as described previously[24]. Briefly, total RNA was extracted using the RNeasy mini kit (Qiagen, Valencia, CA) according to the manufacturer's protocols. RNA (0.5 μg) was reverse transcribed to cDNA using the PrimeScript® RT Master Mix (Takara Bio Inc., Shiga, Japan). The mRNA expression levels were determined using real-time PCR. Real-time PCR was performed with the Thermal Cycler Dice® Real Time System, using the SsoAdvanced™ SYBR® Green Supermix (Bio-Rad Laboratories, Hercules, CA) and normalized to GAPDH mRNA expression. The primer sequences used were as follows: human TGF-β1 forward: 5′-ACT ATT GCT TCA GCT CCA CGG A-3′, reverse: 5′-GGT CCT TGC GGA AGT CAA TGT A-3′; human collagen α1 (I) forward: 5′-ACG AAG ACA TCC CAC CAA TC-3′, reverse: 5′-AGA TCA CGT CAT CGC ACA AC-3′; human GAPDH forward: 5′-GGA GTC AAC GGA TTT GGT-3′, reverse: 5′-AAG ATG GTG ATG GGA TTT CCA-3′; and human TβRI forward: 5′-CTT AAT TCC TCG AGA TAG GC-3′, reverse: 5′-GTG AGA TGC AGA CGA AGC-3′.

Immunofluorescence staining. The cells were grown on eight-well chamber slides or glass bottom dishes and were incubated with HCV virion for 24 hours at 37°C. The cells were washed with PBS, fixed with 4% paraformaldehyde for 10 min at room temperature, and permeabilized with 0.1% Triton X-100 for 20 min at room temperature. After blocking with 3% BSA/10% normal goat serum/PBS for 30 min, the cells were incubated with primary antibodies for 2 hours, followed by incubation with secondary antibodies for 30 min at RT. For detecting NS3 and TβRI on the cell surface, the cells were fixed without permeabilization after incubation with the secondary antibodies. After being washed with PBS, the cells were mounted with Vectashield DAPI mounting medium (Vector Laboratories, Inc., Burlingame, CA) and observed under a Zeiss LSM 700 laser scanning confocal microscope. For quantitative fluorescence analyses, the intensity of phosphorylated Smad3 and the colocalization of NS3 and TβRI (Pearson's colocalization coefficient values) in each panel were calculated with ZEN software.

Proximity ligation assay (PLA). HCV-infected Huh-7.5.1 cells were fixed with 4% paraformaldehyde for 10 min at room temperature and subjected to in situ PLA using a Duolink in situ red starter kit (Olink Bioscience, Uppsala, Sweden) according to the manufacturer's instructions. Briefly, cells were blocked and incubated with primary antibodies against NS3 and TβRI, followed by incubation with the PLA probes, which were secondary antibodies (anti-mouse and anti-rabbit) conjugated to oligonucleotides. DNA ligase was added to enable the formation of circular DNA strands when the PLA probes were in close proximity. This step was followed by incubation with oligonucleotides and polymerase for rolling circle amplification[25]. Texas red-labeled oligonucleotides, which hybridize to the amplified products, were used for visualization. The cells were observed under a Zeiss LSM 700 laser scanning confocal microscope.

Immunoprecipitation and immunoblotting. Anti-FLAG M2 affinity beads were pretreated with 5% bovine serum albumin in 20 mM Tris-HCl, pH 7.5, 150 mM NaCl overnight. Isotype control IgG was bound to Protein G PLUS-Agarose (Santa Cruz) pretreated with 5% bovine serum albumin in 20 mM Tris-HCl, pH 7.5, 150 mM NaCl. Cell lysates with 3xFLAG or 3x-FLAG-NS3 (2 mg protein) were incubated with 50 μl of the beads (10% slurry) at 4°C for 3 hours. The beads were then washed three times with the lysis buffer and incubated with lysates containing 6xHis-TβRI or 6xHis-TβRII (0.5 mg protein) at 4°C overnight. The bound proteins were eluted with the SDS-PAGE sample buffer after washing four times with the lysis buffer and then were subjected to SDS-PAGE (15% acrylamide) followed by transfer onto a PVDF membrane (Pall). The proteins were then visualized using anti-His tag HRP DirectT (MBL, 1/5000) or anti-FLAG BioM2 antibody (Sigma, 10 μg/ml) and horseradish peroxidase-conjugated anti-biotin antibody (Cell Signaling) using the ECL Western blotting detection reagent (GE Healthcare).

In silico docking simulation. The protein-protein docking simulation was implemented based on the geometric complementarity[26] between NS3 protease (PDB ID, 1NS3) and TβRI (PDB ID, 2PJY). Specifically, coordinates of the proteins were projected onto three-dimensional grids separated from each other at regular intervals. A surface score and an intramolecular score were assigned to each grid. This operation was conducted for both the receptor and the ligand. Next, convolution between the obtained grids was performed, the surfaces were explored exhaustively, and the complementarities of the binding states were calculated based on the scores. Amino acid residues appearing frequently in binding states with high complementarity scores can be estimated to be residues that are highly likely to appear in the interaction with an actual receptor. Accordingly, amino acid residues with an interatomic distance of 3.8 Å or less in the putative binding states were defined as contact residues and regarded as the putative contact residues of NS3 and TβRI.

Animal experiment. Chimeric mice with humanized livers were generated as previously described using urokinase-type plasminogen activator (uPA)-transgenic/SCID mice[27]. All mice were transplanted with frozen human hepatocytes obtained from a single donor. All animal experiments were approved by RIKEN Institutional Animal Use and Care Administrative Advisory Committees and were performed in accordance with RIKEN guidelines and regulations. Infection, extraction of serum samples, and euthanasia were performed under isoflurane anesthesia. Male chimeric mice (12- to 14-week old) were intravenously injected with 100 μl HCV J6/JFH-1 strain (1×10^8 copies/ml). Four weeks after HCV inoculation, anti-NS3 antibodies against predicted binding sites with the TβRI receptor were administered at doses of 0.5 mg/kg of BW or 5 mg/kg of BW twice a week for twelve weeks. Normal mouse IgG was administered at a dose of 5 mg/kg of BW as a control. When the animals were euthanized, the livers were either fixed with 4% paraformaldehyde for histological analysis or frozen immediately in liquid nitrogen for mRNA isolation.

Staining of liver tissue sections. The liver tissues were fixed in 4% paraformaldehyde and embedded in paraffin, and tissue sections (6 μm in thickness) were prepared with a Leica sliding microtome (Leica Microsystems, Nussloch, Germany). The liver tissue sections were deparaffinized, rehydrated, and incubated for 5 min with a drop of Proteinase K (Dako Envision) in 2 mL of 0.05 M Tris-HCl buffer (pH 7.5) at room temperature. The liver tissue sections were stained with Mayer's hematoxylin solution (Muto Chemicals) and 1% eosin Y solution (Muto Chemicals). Sirius Red, which results in a red staining of all fibrillar collagen, was used to evaluate fibrosis. Briefly, the liver sections were stained with 0.05% Fast Green FCF (ChemBlink, Inc. CAS: 2353-45-9) and 0.05% Direct Red 80 (Polysciences, Inc. CAS: 2610-10-18) in saturated picric acid (Muto Chemicals) for 90 min at room temperature. The ratios of Sirius Red positive/total area (%) from 6 randomly selected fields were measured for each group using WinROOF software (Mitani Corp., Tokyo, Japan).

Statistics. Statistical analysis was performed using one-way analysis of variance, followed by Dunnett's post-hoc test. A two-tailed Student's *t*-test was used to evaluate differences between the two groups. The Kruskal-Wallis test followed by Dunn's post-hoc test was used for multiple comparisons of Sirius Red positive areas.

1. Marazzi, I. *et al.* Suppression of the antiviral response by an influenza histone mimic. *Nature* **120**, 428–433 (2012).
2. Chaurushiya, M. S. *et al.* Viral E3 ubiquitin ligase-mediated degradation of a cellular E3: viral mimicry of a cellular phosphorylation mark targets the RNF8 FHA domain. *Mol. Cell.* **123**, 352–364 (2012).
3. Tong, M. J., el-Farra, N. S., Reikes, A. R. & Co, R. L. Clinical outcomes after transfusion-associated hepatitis C. *N. Engl. J. Med.* **332**, 1463–1466 (1995).
4. Poynard, T., Yuen, M. F., Ratziu, V. & Lai, C. L. Viral hepatitis C. *Lancet* **362**, 2095–2100 (2003).
5. Lavanchy, D. Chronic viral hepatitis as a public health issue in the world. *Best Pract Res Clin. Gastroenterol.* **22**, 991–1008 (2008).
6. Moradpour, D., Penin, F. & Rice, C. M. Replication of hepatitis C virus. *Nat. Rev. Microbiol.* **5**, 453–463 (2007).
7. Raney, K. D., Sharma, S. D., Moustafa, I. M. & Cameron, C. E. Hepatitis C virus non-structural protein 3 (HCV NS3): a multifunctional antiviral target. *J. Biol. Chem.* **285**, 22725–22731 (2010).
8. Okuno, M. *et al.* Prevention of rat fibrosis by protease inhibitor, Camostat Mesilate, via reduced generation of active TGF-β. *Gastroenterology* **120**, 1784–1800 (2001).
9. Akita, K. *et al.* Impaired liver regeneration in mice by lipopolysaccharide via TNF-α/kallikrein-mediated activation of latent TGF-β. *Gastroenterology* **123**, 352–364 (2002).
10. Ikushima, H. & Miyazono, K. TGFβ signalling: a complex web in cancer progression. *Nat. Rev. Cancer* **10**, 415–424 (2010).
11. Taniguchi, H. *et al.* Hepatitis C virus core protein upregulates transforming growth factor-β1 transcription. *J. Med. Virol.* **72**, 52–59 (2004).
12. Coenen, M. *et al.* Hepatitis C virus core protein induces fibrogenic actions of hepatic stellate cells via toll-like receptor 2. *Lab. Invest.* **91**, 1375–1382 (2011).
13. Wu, C. F., Lin, Y. L. & Huang, Y. T. Hepatitis C virus core protein stimulates fibrogenesis in hepatic stellate cells involving the obese receptor. *J. Cell. Biochem.* **114**, 541–550 (2012).
14. Presser, L. D., Haskett, A. & Waris, G. Hepatitis C virus-induced furin and thrombospondin-1 activate TGF-β1: Role of TGF-β1 in HCV replication. *Virology* **412**, 286–296 (2011).

15. Romano, K. P. *et al.* Molecular mechanisms of viral and host cell substrate recognition by hepatitis C virus NS3/4A protease. *J. Virol.* **85**, 6106–6116 (2011).
16. Kwong, A. D., Kauffman, R. S., Hurter, P. & Mueller, P. Discovery and development of telaprevir: an NS3-4A protease inhibitor for treating genotype 1 chronic hepatitis C virus. *Nat. Biotechnol.* **29**, 993–1003 (2011).
17. Toyoda, M. *et al.* Role of serum soluble Fas/soluble Fas ligand and TNF-α on response to interferon-α therapy in chronic hepatitis C. *Liver* **20**, 305–311 (2000).
18. Lecube, A., Hernandez, C., Genesca, J. & Simo, R. Proinflammatory cytokines, insulin resistance, and insulin secretion in chronic hepatitis C patients: A case-control study. *Diabetes Care* **29**, 1096–1101 (2006).
19. Chouteau, P. *et al.* Hepatitis C virus (HCV) protein expression enhances hepatic fibrosis in HCV transgenic mice exposed to a fibrogenic agent. *J. Hepatol.* **57**, 499–507 (2012).
20. Muller, D. A. & Young, P. R. The flavivirus NS1 protein: Molecular and structural biology, immunology, role in pathogenesis and application as a diagnostic biomarker. *Antiviral Res.* **98**, 192–208 (2013).
21. Zhang, Z. X., Sonnerborg, A. & Sallberg, M. A cell-binding Arg-Gly-Asp sequence is present in close proximity to the major linear antigenic region of HCV NS3. *Biochem. Biophys. Res. Commun.* **202**, 1352–1356 (1994).
22. Alcon, S. *et al.* Enzyme-linked immunosorbent assay specific to Dengue virus type 1 nonstructural protein NS1 reveals circulation of the antigen in the blood during the acute phase of disease in patients experiencing primary or secondary infections. *J. Clin. Microbiol.* **40**, 376–81 (2002).
23. Datta, P. K. & Moses, H. L. STRAP and Smad7 synergize in the inhibition of transforming growth factor beta signaling. *Mol. Cell. Biol.* **20**, 3157–3167 (2000).
24. Tatsukawa, H. *et al.* Role of transglutaminase 2 in liver injury via cross-linking and silencing of transcription factor Sp1. *Gastroenterology* **136**, 1783–1795 (2009).
25. Soderberg, O. *et al.* Characterizing proteins and their interactions in cells and tissues using the *in situ* proximity ligation assay. *Methods* **45**, 227–232 (2008).
26. Katchalski-Katzir, E. *et al.* Molecular surface recognition: determination of geometric fit between proteins and their ligands by correlation techniques. *Proc. Natl. Acad. Sci. USA* **89**, 2195–2199 (1992).
27. Tateno, C. *et al.* Near completely humanized liver in mice shows human-type metabolic responses to drugs. *Am. J. Pathol.* **165**, 901–912 (2004).

Acknowledgments

We are indebted to Mr. Kazushige Katsura and Ms. Chiemi Mishima-Tsumagari (RIKEN Systems and Structural Biology Center, Kanagawa, Japan; Division of Structural and Synthetic Biology, RIKEN Center for Life Science Technologies, Yokohama, Japan) for preparing and providing recombinant NS3, and Dr. Takashi Shimada, Dr. Chise Tateno, and Dr. Masakazu Kakuni (PhenixBio Co., Ltd., Hiroshima, Japan) for helpful discussions regarding the animal experiment. This work was supported in part by a Grant-in-Aid for Scientific Research from the Ministry of Education, Culture, Sports, Science and Technology (23390202 to S.K.), and Grants for Collaborative Researchers from Industries (to K.S.), Program for Drug Discovery and Medical Technology Platforms (to S.K.), and Chemical Genomics Research Program (to S.K.) from RIKEN.

Author contributions

Sakata K., Hara M. and Yaguchi S. performed experiments. Sakata K., Matsuura T., Miyazawa K., Imoto M. and Kojima S. wrote the manuscript. Terada T., Matsumoto T., Shirouzu M., Yokoyama S., Yamaguchi T. and Suzuki T. contributed to the production and the purification of recombinant NS3 and its antibodies. Watanabe N., Aizaki H. and Wakita T. contributed to the production and the purification of HCV and discussion from the point of view of virology. Takaya D. performed docking simulation to predict binding sites. Sakata K. and Kojima S. planned the research. Kojima S. supervised the entire project.

Additional information

Supplementary information accompanies this paper at http://www.nature.com/scientificreports

Competing financial interests: The authors declare no competing financial interests.

How to cite this article: Sakata, K. *et al.* HCV NS3 protease enhances liver fibrosis via binding to and activating TGF-β type I receptor. *Sci. Rep.* **3**, 3243; DOI:10.1038/srep03243 (2013).

ELSEVIER

Institut Pasteur

Microbes and Infection 15 (2013) 45–55

www.elsevier.com/locate/micinf

Original article

Selective estrogen receptor modulators inhibit hepatitis C virus infection at multiple steps of the virus life cycle

Yuko Murakami [a,*], Masayoshi Fukasawa [b], Yukihiro Kaneko [a], Tetsuro Suzuki [c,1], Takaji Wakita [c], Hidesuke Fukazawa [a]

[a] *Department of Bioactive Molecules, National Institute of Infectious Diseases, Toyama 1-23-1, Shinjuku-ku, Tokyo 162-8640, Japan*
[b] *Department of Biochemistry and Cell Biology, National Institute of Infectious Diseases, Tokyo, Japan*
[c] *Department of Virology II, National Institute of Infectious Diseases, Tokyo, Japan*

Received 15 June 2012; accepted 13 October 2012
Available online 23 October 2012

Abstract

We screened for hepatitis C virus (HCV) inhibitors using the JFH-1 viral culture system and found that selective estrogen receptor modulators (SERMs), such as tamoxifen, clomifene, raloxifene, and other estrogen receptor α (ERα) antagonists, inhibited HCV infection. Treatment with SERMs for the first 2 h and treatment 2–24 h after viral inoculation reduced the production of HCV RNA. Treating persistently JFH-1 infected cells with SERMs resulted in a preferential inhibition of extracellular HCV RNA compared to intracellular HCV RNA. When we treated two subgenomic replicon cells, which harbor HCV genome genotype 2a (JFH-1) or genotype 1b, SERMs reduced HCV genome copies and viral protein NS5A. SERMs inhibited the entry of HCV pseudo-particle (HCVpp) genotypes 1a, 1b, 2a, 2b and 4 but did not inhibit vesicular stomatitis virus (VSV) entry. Further experiment using HCVpp indicated that tamoxifen affected both viral binding to cell and post-binding events including endocytosis. Taken together, SERMs seemed to target multiple steps of HCV viral life cycle: attachment, entry, replication, and post replication events. SERMs may be potential candidates for the treatment of HCV infection.

Keywords: HCV; Tamoxifen; SERM (Selective estrogen receptor modulator)

1. Introduction

Over 170 million people in the world are infected with the hepatitis C virus (HCV). Approximately 20% of infected patients develop cirrhosis and hepatocellular carcinoma after chronic HCV infection. No HCV vaccine is available yet, and the current standard of care, which consists of a combination of interferon (IFN) and ribavirin, is only effective for approximately 50% of infected patients, and many patients have serious side effects. Because of the urgent need for novel HCV therapeutics, research is being conducted to develop new anti-HCV drugs. In addition to *in vitro* screening assays that target HCV-specific enzymes, other approaches that use replicon cells and the recently described Huh 7.5.1-JFH-1 (genotype 2a)-infection system have been developed [1]. The Huh 7.5.1-JFH-1-infection system is an excellent system to identify HCV inhibitors that interfere with individual steps of the HCV life cycle, such as viral attachment, entry, and release. This experimental system allows both viral and host components that are involved in HCV infection to be targeted. Although drugs that target the host components may be toxic, such drugs are unlikely to select for resistant viruses.

We screened chemicals using a cell-based screening system [2] and found that tamoxifen and other selective estrogen receptor modulators (SERMs) inhibited HCV infection. Tamoxifen has been successfully used for the treatment of breast cancer since it was found to be an ER antagonist over 30 years ago. Clomifene and raloxifene, which are compounds

* Corresponding author. Tel.: +81 3 5285 1111x2327; fax: +81 3 5285 1272.
E-mail address: murakami@nih.go.jp (Y. Murakami).
[1] Present address: Department of Infectious Diseases, Hamamatsu University School of Medicine, Hamamatsu, Japan.

1286-4579/$ - see front matter © 2012 Institut Pasteur. Published by Elsevier Masson SAS. All rights reserved.
http://dx.doi.org/10.1016/j.micinf.2012.10.003

that are related to tamoxifen, have been developed and used for the treatment of breast cancer and for the treatment of anovulation and osteoporosis. Currently, these three SERMs and toremifene have been approved in Japan and the US, and next-generation SERMs are undergoing clinical evaluation.

Because tamoxifen exhibited the ability to inhibit HCV infection, we determined which SERMs could effectively inhibit HCV infection and be approved for clinical use. The first-generation SERMs—tamoxifen, clomifene, and raloxifene—were all effective against HCV as were other ERα antagonists. We examined whether SERMs could be utilized as new drugs for the treatment of HCV.

2. Materials and methods

2.1. Cells and virus

Human hepatoma cell line, Huh 7.5.1 cells and human embryonic kidney 293T cells were cultured in Dulbecco's modified Eagle's medium (DMEM) (Sigma–Aldrich Co. St. Louis, MO, USA) with 10% fetal bovine serum (FBS). HCV-JFH-1 (HCVcc) (genotype 2a) was the culture supernatant of infected Huh 7.5.1 cells as described previously [2]. A subgenomic replicon cell line, clone #4-1, which harbors the genotype 2a (JFH-1) [3,4], and clone #5-15, that harbors the genotype 1b HCV genome [5], were also cultured in DMEM with FBS.

2.2. Chemicals

The SCADS inhibitor kit I was provided by the Screening Committee of Anticancer Drugs, supported by a Grant-in-Aid for Scientific Research on the Priority Area "Cancer" from The Ministry of Education, Culture, Sports, Science and Technology of Japan. Tamoxifen, diethylstilbestrol, triphenylethylene, 17β-estradiol, and brefeldin A were purchased from Sigma–Aldrich Co. (St. Louis, MO, USA). Clomifene was purchased from LKT Laboratories, Inc. (St. Paul, MN, USA), and hydroxytamoxifen ((*z*)-4-hydroxytamoxifen) and raloxifene were purchased from Enzo Life Sciences, Inc. (Farmingdale, NY, USA). Chloroquine was purchased from WAKO (Osaka, Japan). Other chemicals were purchased from Tocris Bioscience (Bristol, UK).

2.3. Quantification of the viral titer in medium

Huh 7.5.1 cells were seeded in 96-well plates at a density of 2×10^4 cells per well in a volume of 120 μl. The next day, 15 μl of media that contained the test compound and 15 μl of the HCVcc virus stock solution at a moi of 0.01 were added to each well. After 5 days, 100 μl of the culture supernatant was taken from each well, and viral RNA was extracted. Total RNA was also extracted from the cells. Quantitative real-time RT-PCR was then performed with One step SYBR PrimeScript RT-PCR Kit (Takara-Bio Co., Otsu, Japan) as described previously [2]. In the case of #4-1 replicon cell, as an internal control, glyceraldehyde-3-phosphate dehydrogenase (GAPDH) were measured with primers 5′-CCACCCATGGCAAATTCC-3′ and 5′-TGGGATTTCCATTGAT-3′. Cell growth was monitored using the MTT assay as described previously [6].

2.4. Western blotting

Western blotting was performed as previously described [2]. Briefly, cell lysates that contained equal quantities of protein were separated by SDS-PAGE, transferred onto PVDF membranes, and probed with antibodies against the core antigen (2H9), NS5A (Austral Biologicals, San Raman, CA, USA), or GAPDH (Santa Cruz Biotech. Inc., Santa Cruz, USA). After incubation with horseradish peroxidase-conjugated secondary antibodies, the protein bands on the PVDF membranes were detected using an ECL system (GE Healthcare UK Ltd., Amersham Place, UK).

2.5. Production of and infection with pseudo-particles

HCV pseudo-particles (HCVpp) were generated using the following 3 plasmids: a Gag-Pol packaging construct (Gag-Pol 5349), a transfer vector construct (Luc 126), and a glycoprotein-expressing construct (HCV E1E2) (JFH-1, 2a). The generation of the pseudo-particles was performed according to the method described by Bartosch et al. [7]. To express the glycoproteins of other HCV genotypes, HCV E1E2 constructs of the genotypes 1a (H77), 1b (UKN1B 12.6), 2b (UKN2B 2.8), and 4 (UKN4 11.1) were generously provided by Dr. F. Cosset (INSERM, France) [8]. To produce VSVpp, a plasmid that coded the vesicular stomatitis virus (VSV) envelope, pCAG-VSV, was generously provided by Dr. Y. Matsuura (Osaka University, Japan). Gag-Pol 5349 (3.1 μg), Luc 126 (3.1 μg), and each of the individual glycoprotein-expression constructs (1.0 μg) were co-transfected into 293T cells that were seeded on a 10-cm dish (2.5×10^6 cells) using TransIT-LT1 Transfection Reagent (21.6 μl) (Mirus Bio LLC, Madison, WI, USA). The medium from the transfected cell cultures was harvested and used as the pseudo-particle stock. For the infection assay, Huh 7.5.1 cells were seeded onto a 48-well plate at a density of 4×10^4 cells per well one day prior to infection. The medium was then removed, and the cells were subsequently infected with the pseudo-particles in the presence or absence of drug. The cells were then incubated for 3 h. The VSVpp preparation was diluted (1:600) to infect with similar RLU activity compared to the HCVpp. The supernatant was then removed, fresh culture medium was added to the cells, and the cells were incubated for an additional 3 days. The luciferase assays were performed using a luciferase assay system (Promega Co. Madison WI, USA). Anti-CD81 antibody (sc-23962) was purchased from Santa Cruz Biotech.

3. Results

3.1. Tamoxifen and estrogen receptor α antagonists inhibited HCV infection

Using quantitative RT-PCR, we screened the compounds in the SCADS inhibitor kit I. Drugs and HCVcc at a moi of 0.01

were added to Huh 7.5.1 cells. Five days later, the quantity of HCV RNA in the culture supernatant was measured using quantitative real-time RT-PCR [2]. We found that tamoxifen reduced the levels of JFH-1 RNA in the culture supernatant. We also examined the effects of other SERMs and agonists and antagonists of ERα. As shown in Fig. 1, tamoxifen, clomifene, and hydroxytamoxifen, which have a triphenylethylene backbone, exhibited intense inhibitory effects (EC_{50}: approximately 0.1 μM). Triphenylethylene showed reduced inhibitory activity (data not shown). Raloxifene also inhibited viral RNA production at a similar concentration. (EC_{50}: approximately 0.1 μM) (Fig. 1a). Tamoxifen and raloxifene display both ERα antagonist and agonist properties in a dose- and tissue-dependent manner [9]. In contrast, ICI 182,780 (fulvestrant), ZK164015, and MPP (methyl-piperidino-pyrazole) are exclusively antagonistic [10–12]. These ERα antagonists also showed inhibitory activity against JFH-1, but their EC_{50} values were approximately 1 μM (Fig. 1b). As the 50% toxic concentrations (TC_{50}) for these compounds were observed to be greater than 10 μM (Fig. 1a and b), these specific indexes are over 100. In contrast, the ERα agonists 17β-estradiol, diethylstilbestrol, and PPT (1,3,5-tris(4-hydroxyphenyl)-4-propyl-1*H*-pyrozole) did not inhibit HCV (Fig. 1c). As expected, the SERMs that were observed to effectively inhibit HCV RNA production also reduced the core protein levels intracellularly (Fig. 1d).

3.2. SERMs inhibited more than one step of the JFH-1 life cycle

To determine which step of the JFH-1 life cycle was inhibited by the SERMs studied, we performed time-of-addition experiments. As described previously [2], JFH-1 appears to complete one infectious life cycle in approximately 48 h. Huh 7.5.1 cells were inoculated with JFH-1-containing medium (moi 0.1) with or without drug and were then incubated for 2 h. After the medium was removed, fresh medium with or without drug was added. The cells were then incubated for another 46 h. Treatment with 10 μM tamoxifen for 48 h reduced the amount of viral RNA in the medium to 1.7% of levels observed in the control. Treatment with tamoxifen for the first 2 h after infection (0–2 h) reduced viral RNA to 2.3% of the levels observed in the control. The addition of tamoxifen to the fresh medium just after the removal of the virus (2–48 h) resulted in a reduction in the amount of viral RNA to 10.7% of the levels observed in the control. The addition of tamoxifen 24 h after viral inoculation (24–48 h) resulted in a decrease in the amount of viral RNA to 60% of the levels observed in the control (Fig. 2a). This result suggests that tamoxifen inhibits mainly viral entry and some steps during replication. 10 μM of raloxifene exhibited a similar inhibitory pattern but less inhibited by the treatment after the entry step (Fig. 2b). A pure ERα antagonist, ICI 182,780 (30 μM), also exhibited inhibition of both viral entry and the replication steps, but the inhibition of the entry step was not so marked (Fig. 2c).

To further investigate effect on HCV post replication, we infected HCV in the presence of the drugs for 72 h (moi 0.1) and examined their effects on intracellular and extracellular HCV RNA levels. Brefeldin A, an inhibitor of protein transport [13], was used as a positive control of post replication inhibition. In this experimental setting, brefeldin A showed intracellular HCV RNA accumulation suggesting post replication inhibition (Fig. 2d). SERMs generally reduced HCV RNA in cell as well as HCV RNA in medium, although the extent of reduction was different (Fig. 2d). Lower concentration of SERMs reduced extracellular HCV RNA more robustly than intracellular HCV RNA. At a concentration of 0.1 μM, tamoxifen exclusively inhibited HCV RNA in the culture supernatant but not intracellular HCV RNA levels, in a manner similar to that of brefeldin A (Fig. 2d). The results suggest that SERMs inhibit post replication step(s) such as assembly or release. Because low concentrations of tamoxifen failed to inhibit intracellular HCV RNA, SERMs potentially target post replication step(s) more efficiently than replication step. In this condition, higher concentrations (1 and 3 μM) of tamoxifen seemed to inhibit intracellular HCV RNA rather than extracellular HCV RNA, although the reason is not clear.

To determine the effect of these drugs on chronic infection, we used pre-infected Huh 7.5.1 cells. We infected the cell with HCVcc at a moi of 0.01 and incubated for 3 days. Three days after infection, the drugs were added, and the cells were further incubated for 48 h. At the time of drug addition, the cells were persistently infected, and HCVcc was continuously produced and released into the culture supernatant, which is similar condition to chronic infection. HCV RNA was extracted from the culture supernatant and the cells after 48 h and measured copy number of HCV RNA. Both HCV RNA in the culture supernatant and that in the cell were reduced by treatment with the SERMs, but the intracellular HCV RNA levels were less reduced (Fig. 2e). This suggested that the SERMs caused preferential reduction in extracellular HCV RNA through interference with some post replication step(s), such as assembly or release. Brefeldin A accumulated intracellular HCV RNA, and reduced HCV RNA level in the culture supernatant (Fig. 2e).

These data suggested that the SERMs inhibit multiple steps in the HCV life cycle: entry, viral RNA replication and some post replication step(s).

3.3. SERMs inhibited copies and NS5A protein expression in replicon cells

To confirm the effect of these drugs on viral replication, we used two subgenomic replicon cells. The subgenomic replicon cells, derived from Huh7 cells, harbor HCV viral RNA that replicates autonomously, and they express viral proteins. We treated cells that harbored a subgenomic replicon (#4-1, genotype 2a) [3,4] with the SERMs for 48 h and measured the amount of cellular replicon RNA by quantitative RT-PCR. Treatment with 10 μM of tamoxifen, raloxifene, or 3 μM of clomifene, inhibited HCV RNA compare to GAPDH RNA, although statistical significance was shown in only the inhibition of 10 μM of tamoxifen. ICI 182,780 did not show specific inhibition of HCV RNA (Fig. 3a).

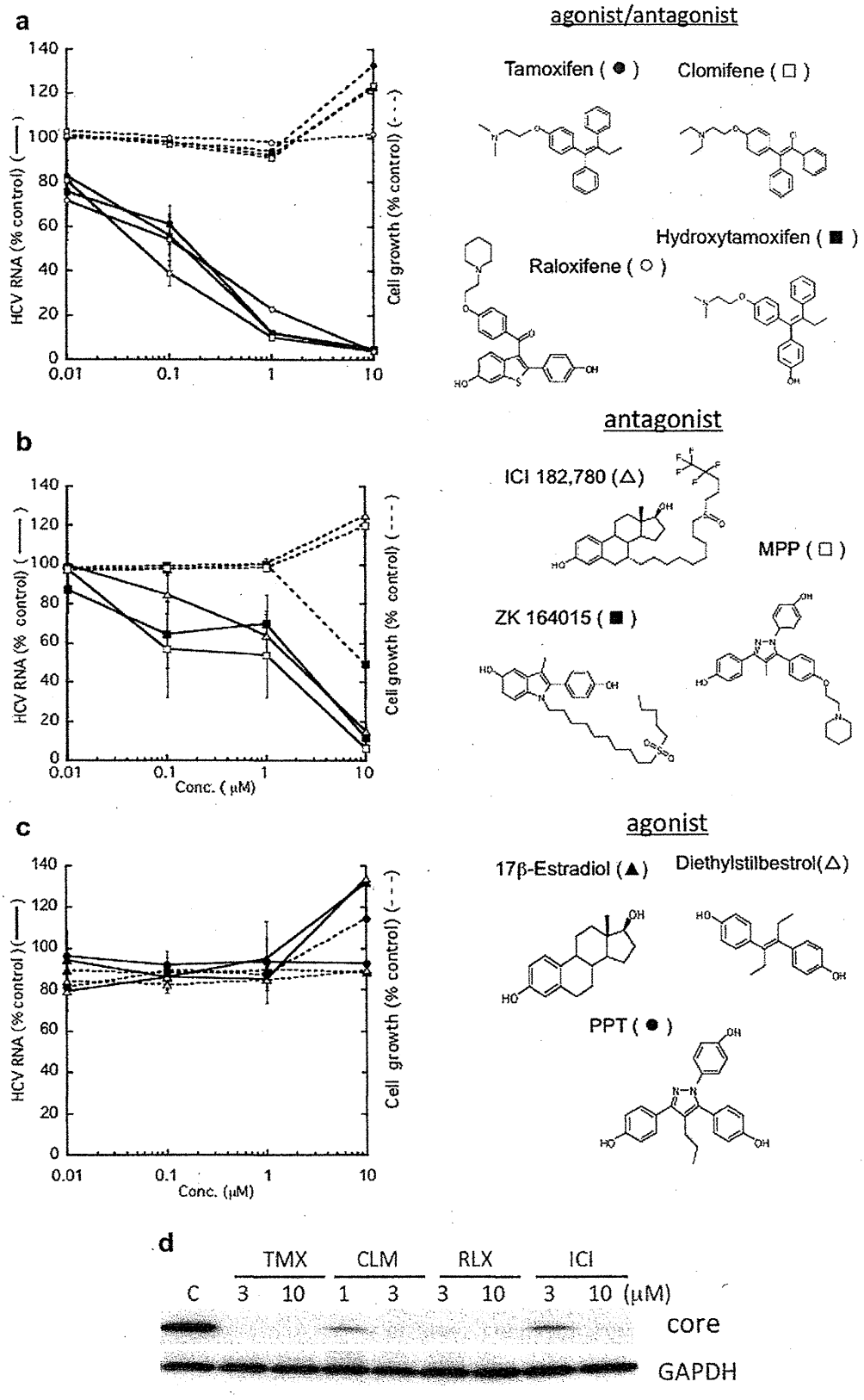

Fig. 1. Effects of SERMs on JFH-1 HCV RNA levels. a) Effects of tamoxifen, clomifene, and raloxifene. Huh 7.5.1 cells were infected with HCV JFH-1 (moi 0.01) in the presence of drugs and were incubated for 5 days. Drugs were added just before viral inoculation. HCV RNA in the medium was measured by tube-capture-RT-PCR [2]. Parallel cultures of cells without virus were analyzed using the MTT assay to detect the inhibition of cell growth due to drug exposure. Tamoxifen (closed circles), clomifene (open rectangles), hydroxytamoxifen (closed rectangles), and raloxifene (open circles). The percentages to control HCV RNA and